LCSQA

Laboratoire Central de Surveillance de la Qualité de l'Air

Note technique

Travaux financés par le ministère chargé de l'environnement

BILAN DES TRAVAUX 2016 DU PROGRAMME CARA

Olivier FAVEZ (INERIS)

SYNTHESE

La présente note synthétise les principaux travaux 2016 du programme CARA, mis en place en 2008, à l'initiative du LCSQA, pour répondre à une forte demande du ministère et des AASQA d'amélioration des connaissances sur les sources et origines des épisodes de pollution particulaire d'ampleur nationale. Basé sur une étroite collaboration avec les AASQA volontaires ainsi qu'avec des laboratoires universitaires, ce programme assure également un transfert de compétences de la recherche vers l'opérationnel.

Afin d'apporter une réponse adaptée au besoin grandissant de compréhension immédiate de ces épisodes, le programme CARA s'est attaché au cours de ces dernières années au développement d'un dispositif d'observation en temps réel de la composition chimique des PM. Ce dispositif, unique en Europe, a notamment permis de mettre en évidence le rôle majeur joué par les émissions locales de combustion (chauffage et transport routier) dans la survenue d'un épisode de pollution persistant au cours des trois premières semaines de décembre 2016.

Par ailleurs, un travail de veille bibliographique sur les travaux de recherche récents indique une utilisation accrue des outils statistiques de type « modèle sources-récepteur » pour l'identification et la quantification des sources de particules fines dans l'air ambiant en France. En particulier, les méthodes de type *Positive Matrix Factorization* (PMF) sont aujourd'hui fortement utilisées par différents laboratoires universitaires, notamment en collaboration avec le LCSQA et les AASQA. Ce travail de veille a été co-financé par l'ADEME dans le cadre du projet SOURCES.

Enfin, une analyse approfondie de 15 jeux de données obtenus pour des sites du dispositif national de surveillance de la qualité de l'air a également été réalisée dans le cadre de ce programme. Ce travail a notamment permis de consolider la connaissance des principales sources chroniques de PM en fond urbain à l'échelle nationale.

REF. INERIS : DRC-16-159637-12362A

1. CONTEXTE

Le programme CARA, « caractérisation chimique des particules », a été mis en place en 2008, en réponse au besoin de compréhension et d'information sur l'origine des épisodes de pollution particulaire mis en évidence par les pics de PM_{10} du printemps 2007. Créé et géré par le LCSQA, ce dispositif aujourd'hui pérenne, fonctionne en étroite collaboration avec les AASQA volontaires et, ponctuellement, avec des laboratoires universitaires [1]. Il a pour principaux objectifs de :

- Déterminer les principales sources de PM tant en « situation normale » que lors des épisodes de pollution, afin d'aider à l'élaboration de plans d'actions adaptés.
- Apporter un appui technique et scientifique aux AASQA dans la mise en œuvre de campagnes de spéciation chimique des PM (dont mesures automatiques).
- Elaborer des guides méthodologiques et protocoles d'assurance et contrôle qualité pour différentes techniques d'intérêt pour la spéciation chimique des PM et les études de sources.
- Réaliser un retour d'expérience et assurer une veille scientifique sur les méthodologies et projets visant l'amélioration des connaissances.
- Réaliser des exercices de Comparaisons Inter-Laboratoires (CIL) pour la mesure des espèces chimiques (majeures et traces).
- Optimiser les modèles de chimie-transport via des exercices de comparaison des mesures aux sorties de modèles, afin de permettre une meilleure anticipation des épisodes de pollution particulaire.

D'un point de vue pratique, ce programme repose historiquement sur l'analyse chimique au laboratoire (INERIS, IMT Lille-Douai ou laboratoires universitaires) de filtres collectés en plusieurs points du dispositif national. Ces prélèvements sont réalisés par les AASQA volontaires, principalement en PM_{10} et sur sites de fond urbain. Ils sont effectués de façon quasi-continue (typiquement, en alternance avec les filtres pour la surveillance réglementaire des HAP) tout au long de l'année, mais ne sont analysés qu'en fonction de leur intérêt (« situations d'urgence », ou utilisation dans le cadre d'une étude ou d'un programme de recherche). Néanmoins, l'utilisation exclusive de prélèvements sur filtres et l'analyse différée ne permet pas de bien répondre au besoin grandissant d'une détermination en temps quasi-réel de la composition chimique des PM. Le développement d'analyseurs automatiques dimensionnés pour la surveillance opérationnelle (en particulier l'Aethalomètre multi-longueur d'onde AE33 et l'Aerosol Chemical Speciation Monitor : ACSM) permet aujourd'hui de compléter ce dispositif « sur filtres ». En effet, suite aux travaux de veille technologiques et de recherche menés par l'INERIS en collaboration avec le Laboratoire des Sciences du Climat et de l'Environnement (LSCE) au SIRTA [2-3], le programme CARA dispose depuis 5 ans de données de spéciation chimique des particules submicroniques en Ile de France. Sur la base de ces travaux, le LCSQA a également pu accompagner les AASQA dans l'implantation d'analyseurs automatiques au sein du dispositif national [3-5], qui dispose aujourd'hui d'un réseau opérationnel d'observation en temps réel de la composition chimique des particules unique en Europe.

Depuis 2015, les actions relatives au suivi et à l'optimisation de l'utilisation des analyseurs automatiques de la composition chimique des PM sont intégrées à la thématique « assurance qualité » du programme des travaux du LCSQA. Ces actions sont donc décrites en dehors du cadre de la présente note (e.g., [6]). Cette dernière rend compte des actions

réalisées en 2016 pour l'amélioration des connaissances sur la nature des PM. Elle traite plus spécifiquement de la caractérisation chimique de l'épisode de pollution de Décembre 2016, des méthodologies d'estimation de sources de PM, et du travail de veille bibliographique sur les travaux de recherche récents ou en cours à l'échelle nationale. Des exemples de valorisation des travaux du programme CARA via la publication d'articles scientifiques et la participation à des conférences internationales est également présentée en Annexe de la présente note.

2. CARACTERISATION CHIMIQUE DES EPISODES DE POLLUTION PARTICULAIRE

Cette action permet d'apporter des informations sur l'origine des particules, en situation de fortes concentrations à partir de données automatiques et/ou d'échantillons collectés sur les sites du dispositif CARA. En 2016, la mobilisation du dispositif CARA dans ce contexte a concerné l'épisode de pollution du mois de Décembre [7]. En effet, alors qu'aucun épisode majeur persistant et d'ampleur national n'avait été observé en fin d'hiver - début de printemps (contrairement aux années précédentes), de nombreuses régions métropolitaines (en particulier celles de la moitié nord de la France, Auvergne-Rhône-Alpes et Nouvelle Aquitaine) ont connu des niveaux de PM_{10} avoisinant ou dépassant les seuils d'information (50µg/m^3) et d'alerte (80µg/m^3) au cours des trois premières semaines du mois de décembre 2016.

De façon similaire à ceux de décembre 2013 [3], ces épisodes de début d'hiver se sont développés lors de situations météorologiques très stables (régime anticyclonique) propices à l'accumulation des polluants, les faibles températures conduisant en outre à une importante utilisation du chauffage résidentiel. Cette conjonction est à l'origine des fortes teneurs en matière carbonée dans les particules observées en temps réel (Figure 1).

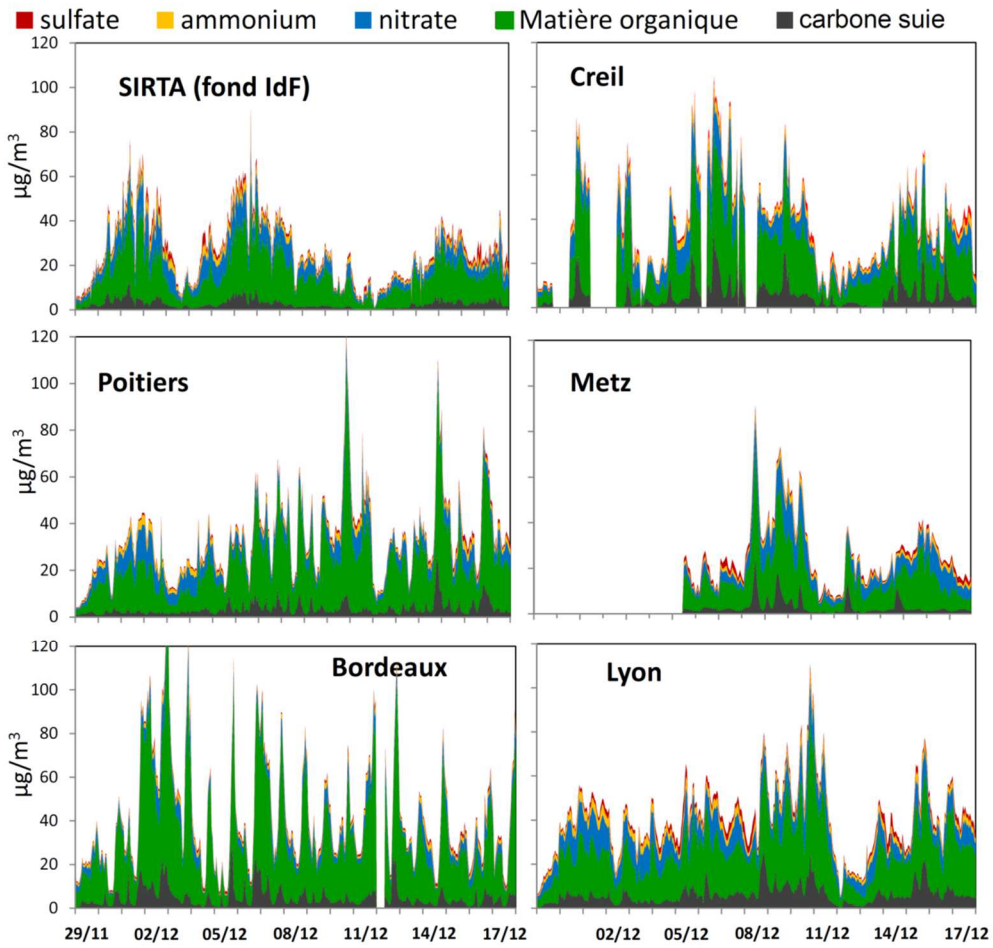

Figure 1 : Variations temporelles des espèces chimiques majeures des particules fines sur 6 sites de fond (péri-)urbain du dispositif CARA. Mesures ACSM (en PM1) et AE33 (en PM2.5) lors des 3 premières semaines de déc. 2016. (courbes empilées)

Malgré le caractère global des conditions météorologiques, des spécificités locales d'émission peuvent expliquer les fortes variations observées d'une région à une autre. Les résultats issus des analyseurs automatiques de la composition chimique des particules fines (AE33 et ACSM) convergent vers une influence majeure des émissions locales, i.e. combustion de biomasse (chauffage domestique) et transport routier, sur les niveaux de particules mesurés. Enfin, et dans une moindre mesure, une contribution de nitrate d'ammonium, formé via des mécanismes photochimiques, a également été observée sur le nord et l'est de la France. L'origine potentielle de ces aérosols inorganiques secondaires a été approfondie début 2017 par analyse isotopique de l'azote (d15N) présent au sein de l'ammonium prélevé sur filtres. Les résultats obtenus suggèrent une origine majoritairement liée aux activités de combustion (transport routier, chauffage, industries), plutôt qu'aux activités agricoles, pour expliquer ces concentrations non négligeables de nitrate d'ammonium. [8]

Par ailleurs, en 2016, les activités de comparaisons mesures/modèles (Chimere) ont porté sur l'analyse de l'épisode de pollution de mars 2015. Les résultats obtenus ont été intégrés à une publication scientifique internationale dédiée à l'étude de cet épisode printanier, reproduite en Annexe 1 du présent rapport. Ces résultats confirment les difficultés d'une bonne prévision des concentrations de la matière organique (avec des biais négatifs pour le modèle de l'ordre de 60-80%), en lien notamment à la prédominance de la fraction secondaire. Une meilleure prise en compte des émissions primaires carbonées reste cependant également nécessaire, comme illustré par des biais significatifs sur les concentrations de carbone suie (de l'ordre de -70% à +70% selon les sites). Les fortes concentrations d'aérosols inorganiques secondaires (nitrate et sulfate d'ammonium) de cet épisode printanier sont quant à elles globalement bien reproduites par le modèle.

3. VEILLE BIBLIOGRAPHIQUE SUR LES ETUDES DE SOURCES DE PM

Cette action correspond à la mise à jour du rapport de veille bibliographique sur les études scientifiques visant l'identification et la quantification des sources de particules fines dans l'air ambiant (PM_{10} et $PM_{2,5}$) en France. Plus spécifiquement, elle traite des travaux de recherche impliquant des AASQA et/ou le LCSQA, et porte l'accent sur la mise en œuvre de méthodologies de traitement de données expérimentales pour l'amélioration des connaissances sur les sources anthropiques en milieu urbain au cours des dix dernières années [9]. Ce travail est également intégré au projet SOURCES, co-financé par l'ADEME (2014-2017).

Cette étude a permis de dresser un bilan des pratiques méthodologiques concernant l'étude des sources de PM via l'étude de leur composition chimique. Le tableau ci-après synthétise les principaux outils de traitement de données utilisés dans les différents projets recensés.

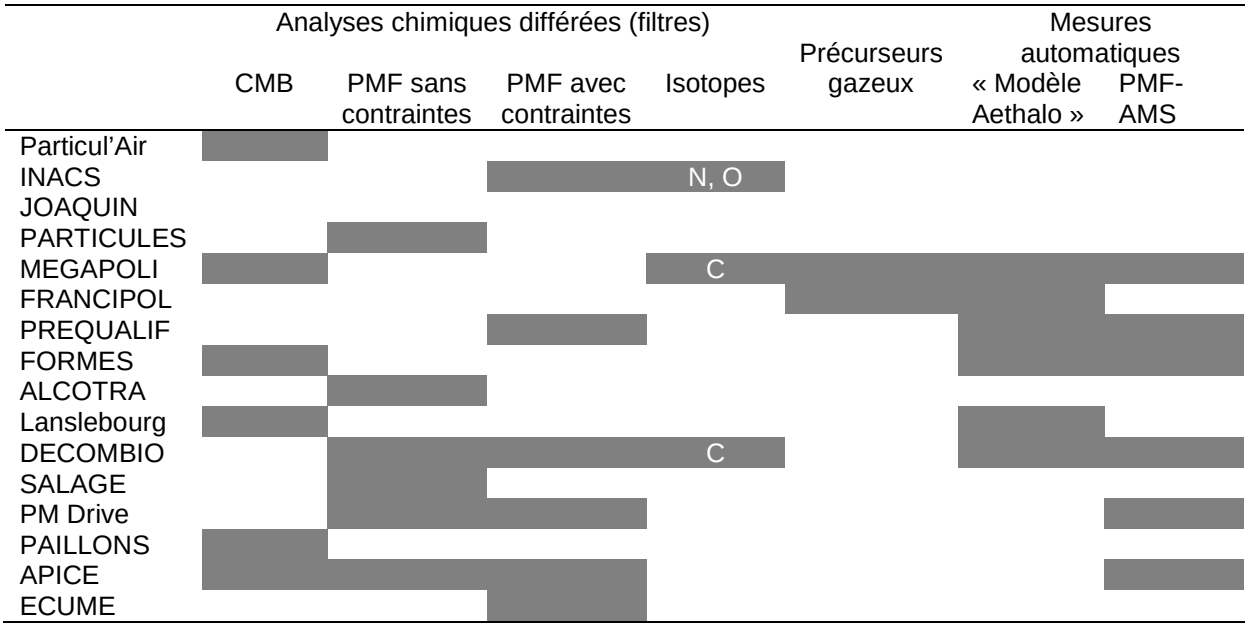

On constate tout d'abord que l'ensemble de ces projets met en œuvre des méthodologies de traitement de données relativement élaborées, dépassant l'utilisation des approches mono-traceurs (se focalisant sur une source unique d'émission). Ces méthodologies incluent notamment la détermination très étendue des constituants de la matière particulaire, via la détermination d'une grande diversité de traceurs spécifiques, suivie de l'utilisation d'outils statistiques. Ces derniers sont basés soit sur une connaissance a priori des principales sources locales/régionales et de leur profil d'émission (par ex. CMB : « Chemical Mass Balance »), soit sur une détermination a posteriori de ces sources à l'aide de profils d'émission déterminés par ailleurs (PMF sans/avec contraintes). Si l'outil CMB est historiquement le plus utilisé, les projets les plus récents ont plutôt tendance à se baser sur les approches de type PMF. Ces dernières présentent l'avantage de ne pas dépendre de la robustesse d'hypothèses de départ sur le nombre et la nature des sources à quantifier.

Compte-tenu de l'importance des coûts d'obtention des jeux de données d'entrée, les études mettant en œuvre la PMF ne peuvent être que ponctuelles (dans l'espace et/ou dans le temps). Néanmoins, les différents programmes et projets de recherche mis en œuvre ces dernières années ont permis à la France de combler son retard dans l'utilisation de l'outil

PMF par rapport à ses voisins européens, avec plus de vingt sites concernés par des travaux d'échelle (pluri-)annuelle sur les sources de PM pour la période 2012-2016, contre seulement 2 étude de ce type recensées avant 2012 (Figure 2).

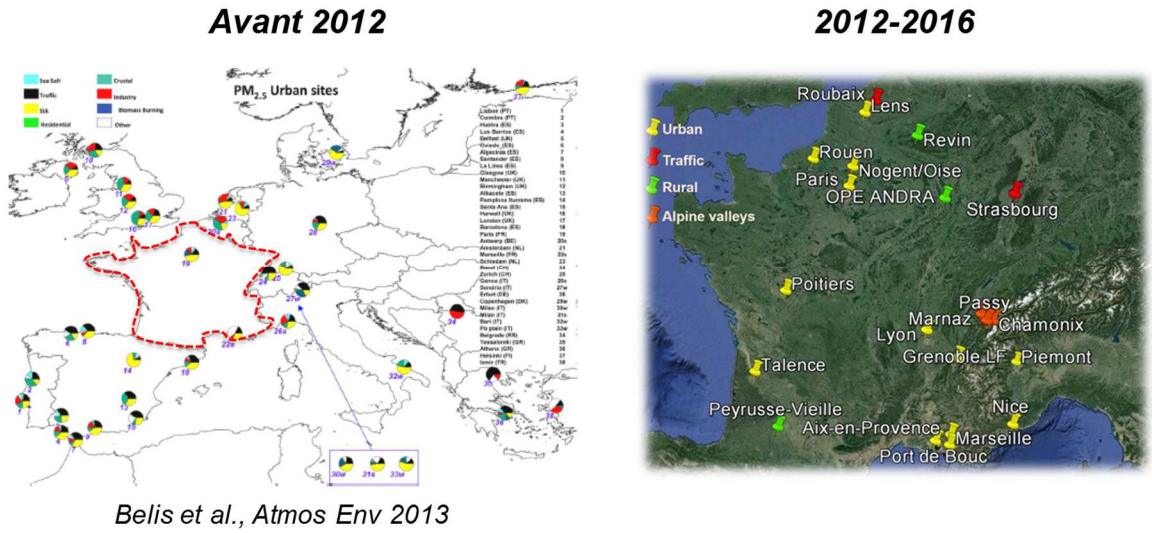

Figure 2 ***Localisation des sites récepteurs français instrumentés (avant/après 2012) pour la réalisation d'études de sources via des approches de type PMF à partir de la caractérisation chimique de prélèvements sur filtres.***

Les mesures des isotopes stables de différents constituants de la phase particulaire (e.g., ^{14}C ou ^{15}N, comme dans le cas de DECOMBIO et d'INACS respectivement) permettent d'apporter des informations sur la nature des précurseurs gazeux ayant conduit à la formation des aérosols secondaires. Néanmoins, en raison des coûts élevés d'analyse et de la faible disponibilité des quelques chaînes analytiques dédiées à ce type de mesures, ces méthodologies ne sont encore que trop peu utilisées.

On note également la fréquence d'utilisation des méthodologies basées sur la mesure automatique, i.e., fractions du Black Carbon via le modèle Aethalomètre, et analyse PMF sur les spectres de masse de la matière organique analysée à l'aide d'*Aerosol Mass Spectrometer* (AMS) ou d'*Aerosol Chemical Speciation Monitor* (ACSM).

Le succès du modèle Aethalomètre repose notamment sur sa facilité de mise en œuvre (instrumentation simple et robuste, coûts d'investissement et de maintenance limités), ainsi que sur son aptitude à bien rendre compte de l'influence des certaines activités humaines (en particulier combustion de biomasse). En revanche, il n'apporte aucune information sur les autres sources d'émission primaires (e.g., discrimination des activités industrielles, poussières naturelles) ni sur l'importance des mécanismes de formation secondaire (en particulier la fraction inorganique).

Si les mesures AMS permettent de documenter les espèces majeures de l'aérosol submicronique (classe de taille fortement influencée par les émissions anthropiques) et d'obtenir de précieuses informations sur les différentes familles d'aérosols organiques (primaires et secondaires), l'utilisation de cet instrument reste limitée à des campagnes intensives (e.g., MEGAPOLI, FORMES, DECOMBIO, PM Drive) en raison de son coût de mise en œuvre. Ainsi, les informations tirées de cet instrument concernent des périodes assez limitées dans le temps (de l'ordre de quelques semaines) et ne permettent de documenter

les contributions annuelles moyennes et tendances. L'émergence et le déploiement des mesures par ACSM (plus robuste et moins onéreux, mais moins sensible, que l'AMS), notamment dans le cadre des programmes ACTRIS (infrastructure de recherche européenne) et CARA, permet aujourd'hui de dépasser ces limitations. Cependant, le traitement de données par approche PMF sur de très grands jeux de données n'est pas trivial et nécessite une utilisation optimisée des outils statistiques disponibles. Ce travail de développement méthodologique est aujourd'hui en cours au sein de la communauté scientifique internationale.

4. ESTIMATION DES SOURCES DE PM A L'AIDE D'OUTILS STATISTIQUES

La construction et l'évaluation de plans d'action pour la réduction des émissions des principales sources anthropiques nécessite d'identifier et de quantifier ces sources aussi finement que possible. Deux grands types de méthodologies sont principalement utilisées : (i) celles se basant sur l'utilisation de modèles numériques permettant de simuler le devenir des polluants dans l'atmosphère à partir de cadastres d'émission et de la paramétrisation des conditions météorologiques et des processus physico-chimiques de (trans-)formation des PM ; (ii) celles se basant sur la mesure de la composition chimique (et/ou de la granulométrie) des particules sur un site récepteur et l'utilisation de traceurs spécifiques aux différentes sources étudiées. Si les modèles numériques doivent permettre d'apporter des informations en tout point du territoire et selon des échelles temporelles aussi larges que souhaité, leur validation nécessite des comparaisons avec les résultats obtenus par la mise en œuvre de méthodologies expérimentales.

A ce titre, l'outil statistique *Positive Matrix Factorization* (PMF) est utilisé depuis 2011 par le LCSQA pour l'exploitation des données issues du programme CARA et des travaux sur les HAPs [3, 10-13]. Il permet la détermination de la contribution des principales sources et mécanismes de formation des polluants, à partir d'un jeu de données aussi dense que possible, en termes de nombre d'échantillons et d'espèces chimiques mesurées [14].

Les informations fournies par ce type d'approche sont facilement exploitables (et communicables) sur les sources primaires de particules (e.g., combustion de biomasse, émissions directes à l'échappement automobile, sels de mer, …). En revanche, les sorties PMF incluent également des facteurs correspondant à différentes familles d'aérosols secondaires (absentes des analyses CMB), provenant de précurseurs gazeux dont les sources restent à déterminer. En outre, comme les processus de transformations secondaires ne sont généralement pas linéaires, les polluants émis par les différentes sources (anthropiques ou naturelles) réagissent tous entre eux selon des processus que les modèles récepteurs ne peuvent pas réellement discriminer ni quantifier. Pour exemple, les sorties PMF permettent d'estimer la contribution des émissions directes de particules par le transport routier, mais n'apportent pas d'information chiffrée sur l'influence réelle de cette source dans la formation d'aérosols secondaires (en particulier le nitrate d'ammonium et aérosols organiques secondaires).

Il est également important de souligner que :

1) ce type d'outil ne permet pas d'étudier directement l'origine géographique des principales sources d'émissions identifiées. Néanmoins, le couplage des résultats obtenus avec une analyse des conditions météorologiques et/ou de rétro-trajectoires des masses d'air peuvent permettre d'apporter des informations qualitatives sur ces origines géographiques ;

2) compte-tenu de la non-linéarité des mécanismes atmosphériques mis en jeu, les estimations de contributions de sources ne reflètent pas directement le niveau de réduction des concentrations pouvant être atteint par les plans d'action. Ainsi, les résultats obtenus à l'aide de ces méthodologies expérimentales ne peuvent être utilisées simplement pour la réalisation de scénarii pour l'étude d'impacts de l'efficacité de telle ou telle mesure de réduction des émissions.

Dans les deux cas discutés ci-dessus (i.e., étude des origines géographiques et efficacité réelle de la réduction des émissions sur les niveaux de concentrations de PM en air ambiant),

le recours à la modélisation numérique, basée sur les inventaires d'émission, une bonne connaissance des conditions météorologiques, et la paramétrisation des phénomènes de (trans-)formation des aérosols, est indispensable. La validation de ce type d'approche passe cependant par la comparaison des résultats obtenus aux données de composition chimique et de contributions de sources primaires déterminées à l'aide des méthodologies expérimentales étudiées dans le cadre du présent projet. En effet, basées sur l'observation, ces méthodologies expérimentales rendent compte de situations réelles, auxquelles les simulations numériques doivent pouvoir se confronter.

En parallèle de l'expansion rapide au sein de la communauté scientifique des outils statistiques de traitement de données expérimentales pour l'étude des sources de PM (cf. section 3 du présent rapport), cette thématique a récemment (mi-2014) été retenue comme nouveau sujet de travail du comité européen de normalisation (CEN TC 264). Egalement sous l'impulsion du Joint Research Center (JRC), le forum FAIRMODE (réunissant la communauté de modélisateurs à l'échelle européenne) intègre désormais l'organisation d'exercices d'intercomparaisons de résultats issus de modèles récepteurs. De même, les programmes européens EMEP et ACTRIS articulent certaines de leurs activités autour du développement et/ou de l'évaluation de méthodologies expérimentales d'attribution de sources (e.g., campagnes de mesure axées sur le modèle Aethalomètre à l'hiver 2017-2018, méthodologies de traitement de données ACSM, …). Néanmoins, il n'existe à ce jour aucune méthodologie normalisée d'estimation des sources de PM en air ambiant,

Outre les différences pouvant être observées d'une approche à l'autre, l'exploitation d'un même jeu de données à l'aide de la même méthode ne garantit pas l'obtention de résultats similaires par différents utilisateurs [9, 15]. En effet, l'utilisation de ces outils statistiques revêt une part de subjectivité, notamment liée au choix des hypothèses de départ et/ou de la solution finalement retenue. Ainsi, la comparaison de résultats issus de différentes études basées sur une même approche contient une part d'incertitude liée aux inhomogénéités de traitement de données. Dans ce contexte, une ré-analyse PMF par traitement harmonisé de jeux de données disponibles à l'échelle nationale a été proposée et réalisée dans le cadre du projet SOURCES (co-financé par l'ADEME, 2014-2017).

Cette dernière étude inclut le développement d'une méthodologie de traitement de données harmonisée (analyse statistique du jeu de données, sélection des variables d'entrée pour l'analyse PMF, estimation de leurs incertitudes, application des contraintes chimiques spécifiques dans les profils chimiques de certains facteurs). Cette méthodologie a ensuite été appliquée à une quinzaine de jeux de données collectées ces dernières années dans le cadre du programme CARA et/ou de projets de recherche nationaux/européens. Les jeux de données utilisés ont été sélectionnés de façon à disposer d'un panel aussi large que possible et comparable en termes de nombre d'échantillons, de durée d'étude, et de résultats de spéciation chimique des PM_{10}. Ils sont principalement issus de prélèvements réalisés par les AASQA sur des sites de fond urbain (cf. Annexe 2).

Les résultats obtenus lors de cette étude sont repris et discutés dans un rapport spécifique [16]. Ces résultats convergent vers les principales conclusions suivantes :

✓ Les émissions primaires liées au transport routier influencent fortement la masse des PM_{10} sur les sites de proximité automobile, mais également sur certains sites de fond urbain tels que Rouen, Marseille, Grenoble et Nogent (avec des contributions relatives de l'ordre de

20-30% en moyenne annuelle). Sur les autres sites, les contributions annuelles sont d'environ 10%.

✓ La source de combustion de la biomasse est très importante en hiver, contribuant jusqu'à 70% de la masse des PM_{10} en moyenne saisonnière à Chamonix (contre 10-15% à Marseille, Lens et Rouen, et environ 30% sur tous les autres sites).

✓ Les aérosols secondaires riches en nitrate d'ammonium présentent une concentration maximale au printemps (typiquement 30% des PM_{10}), en particulier sur les sites de la moitié nord de la France.

✓ L'impact des aérosols secondaires riches en sulfate d'ammonium sur les niveaux de PM_{10} est observée en période estivale (en particulier dans le sud de la France).

✓ Les poussières minérales présentent des contributions importantes et relativement comparables au printemps et en été sur un grand nombre de sites.

✓ De nouveaux traceurs organiques (e.g., polyols et MSA : acide méthylsulfonique) rarement utilisés dans les études précédentes ont permis la quantification de sources biogéniques spécifiques (e.g., émissions primaires et aérosols organiques secondaires d'origine marine, respectivement), de contributions non-négligeables du printemps à l'automne.

✓ Le facteur industriel identifié sur seulement 5 des 15 sites étudiés présente une variabilité spatiale inhomogène. Il reste cependant difficile de bien isoler cette source. Il en est de même pour les résidus de combustion de fioul lourd (incluant notamment les émissions du transport maritime).

A titre de synthèse et d'illustration de ces principales conclusions, la Figure 3 présente les contributions moyennes des principales sources de PM à l'échelle nationale en fond urbain, obtenus en combinant les résultats issus de l'analyse PMF harmonisée pour les 10 agglomérations suivantes : Rouen, Nogent sur Oise, Lens, Poitiers, Lyon, Grenoble, Bordeaux, Aix en Provence, Marseille, et Nice.

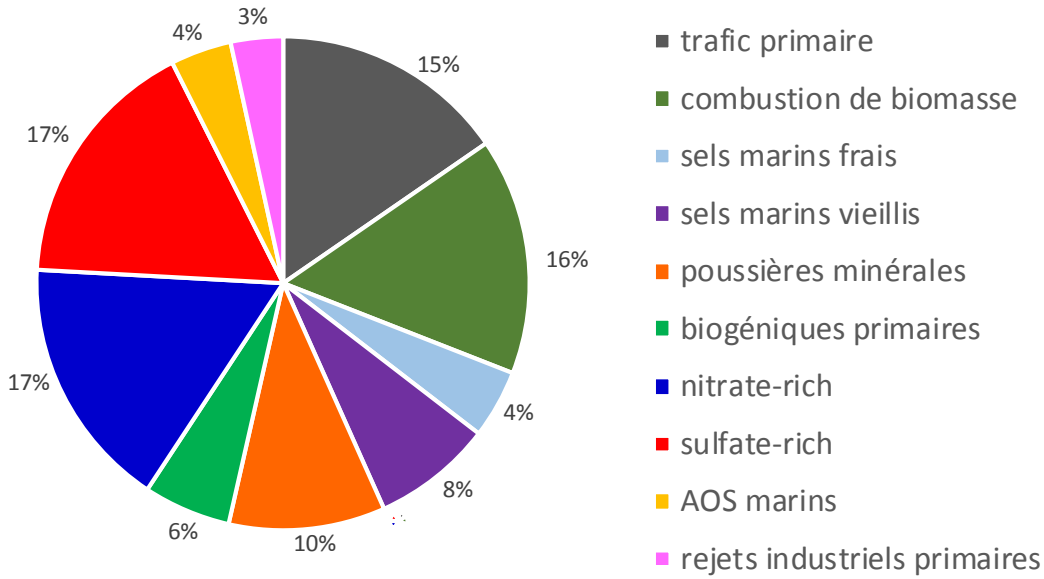

Figure 3 : Contributions annuelles moyennes des principaux facteurs constitutifs des PM_{10} en fond urbain à l'échelle nationale (Moyenne des résultats obtenus par analyse PMF harmonisée sur 10 sites de fond urbain du projet SOURCES).

Une limitation inhérente à l'utilisation d'un protocole de traitement de données harmonisé réside dans la restriction et la fiabilité du panel des espèces chimiques utilisées comme variables d'entrée. Ainsi, selon les caractéristiques spécifiques des sites et jeux de données étudiés, l'utilisation d'une approche « personnalisée » de traitement de données peut être préférée. En particulier, l'élargissement du jeu de données d'entrée avec, par exemples, de nouveaux marqueurs organiques (e.g., n-alcanes, hopanes, cellulose, oxy- et nitro-HAP dérivés, et/ou autres marqueurs de composés secondaires), des résultats de mesures isotopiques (e.g., ^{14}C, ^{15}N), et/ou des données d'analyseurs automatiques (e.g., AE33, ACSM, mesures de métaux en continu), doit permettre d'améliorer l'identification et la quantification de certaines sources minoritaires (e.g., émissions industrielles et/ou combustion de fioul lourd) ainsi que les facteurs liés aux aérosols secondaires.

Les perspectives d'utilisation future des résultats obtenus dans le cadre de cette étude incluent notamment :

- Le couplage des sorties PMF avec des données de rétro-trajectoires de masses d'air, permettant à terme d'identifier les zones géographiques potentielles d'émissions des sources de PM.
- La comparaison des résultats obtenus avec les inventaires d'émission et des sorties de modèles numériques de type CTM (*Chemical Transport Model*).
- La mise en regard des sources de PM identifiées et de leur impact sanitaire potentiel avec l'utilisation par exemple du potentiel oxydant des PM (voir de tests cellulaires) comme nouvelle métrique d'évaluation de la qualité de l'air.

A noter que les travaux 2016 ont également porté sur la finalisation de l'étude PMF sur 5 sites du nord de la France sur la période 2013-2014 dans le cadre de la thèse de doctorat de Diogo Oliveira [17] (sur financements LCSQA/INERIS et IMT Lille-Douai), ainsi que sur l'analyse des sources de PM_{10} pour l'année 2015 à la station de fond urbain de Poitiers *Augouard* en collaboration avec Atmo Poitou-Charentes [18].

5. METHODOLOGIES D'ESTIMATION DES SOURCES EN TEMPS REEL

Si le déploiement d'analyseurs automatiques de type ACSM en différents points du dispositif national permet de renseigner en temps réel la composition chimique de la fraction submicronique des particules (cf. section 2), il n'existe pas aujourd'hui d'outil automatisé de traitement de données délivrant une estimation en temps quasi-réel de l'influence des principales sources d'émission. Ce travail d'interprétation des données en temps réel nécessite le développement des méthodologies novatrices et adaptées aux jeux de données produits par l'instrumentation utilisée (AE33 et ACSM). L'analyse en temps réel de l'épisode de pollution de décembre 2016 a permis de mettre en œuvre une première procédure de traitement de données permettant de dissocier la contribution des émissions de combustion des autres constituants particulaires [7]. Cette procédure intègre les deux étapes ci-dessous :

1) Analyse des données AE33 : les mesures AE33 permettent de distinguer deux fractions du Black Carbon (BC), que l'on peut relier à la combustion d'hydrocarbures (BC_{ff}) et à la combustion de biomasse (BC_{wb}). Ces fractions peuvent ensuite être utilisées pour estimer (à l'aide d'un facteur multiplicatif et avec une précision de l'ordre de ± 50%) les concentrations de PM_{10} attribuables aux deux familles de sources (notées respectivement PM_{ff} et PM_{wb}), tel que :

$$PM_{ff} = a \times BC_{ff}$$

$$\text{Et } PM_{wb} = b \times BC_{wb}$$

où PM_{ff} et PM_{wb} représentent la concentration massique de particules PM_{10} issues respectivement de la combustion d'hydrocarbures et de la combustion de biomasse. Outre le BC, PM_{ff} et PM_{wb} sont constituées principalement d'aérosols organiques primaires. Les coefficients *a* et *b* sont issus (i) de la littérature scientifique pour la contribution fossile, et (ii) d'études LCSQA précédentes pour la contribution biomasse [13, 19].

A noter que les émissions primaires à l'échappement automobile sont comprises au sein de la fraction liée à la combustion d'hydrocarbures (PM_{ff}), mais que ces estimations n'intègrent pas les émissions hors-échappement, i.e., particules issues de l'abrasion de la chaussée, des pneus, des freins, etc. Ces estimations ne tiennent pas non plus compte de l'influence de l'échappement automobile sur la formation d'aérosols secondaires à partir des émissions de précurseurs gazeux (i.e., NO_x, issus à 60% du transport au niveau national), dont l'influence sur les PM_{10} est impossible à évaluer à partir de mesures en temps réel.

La Figure 4 permet d'illustrer les résultats obtenus à l'aide de cette méthodologie au cours de l'épisode de pollution de décembre 2016.

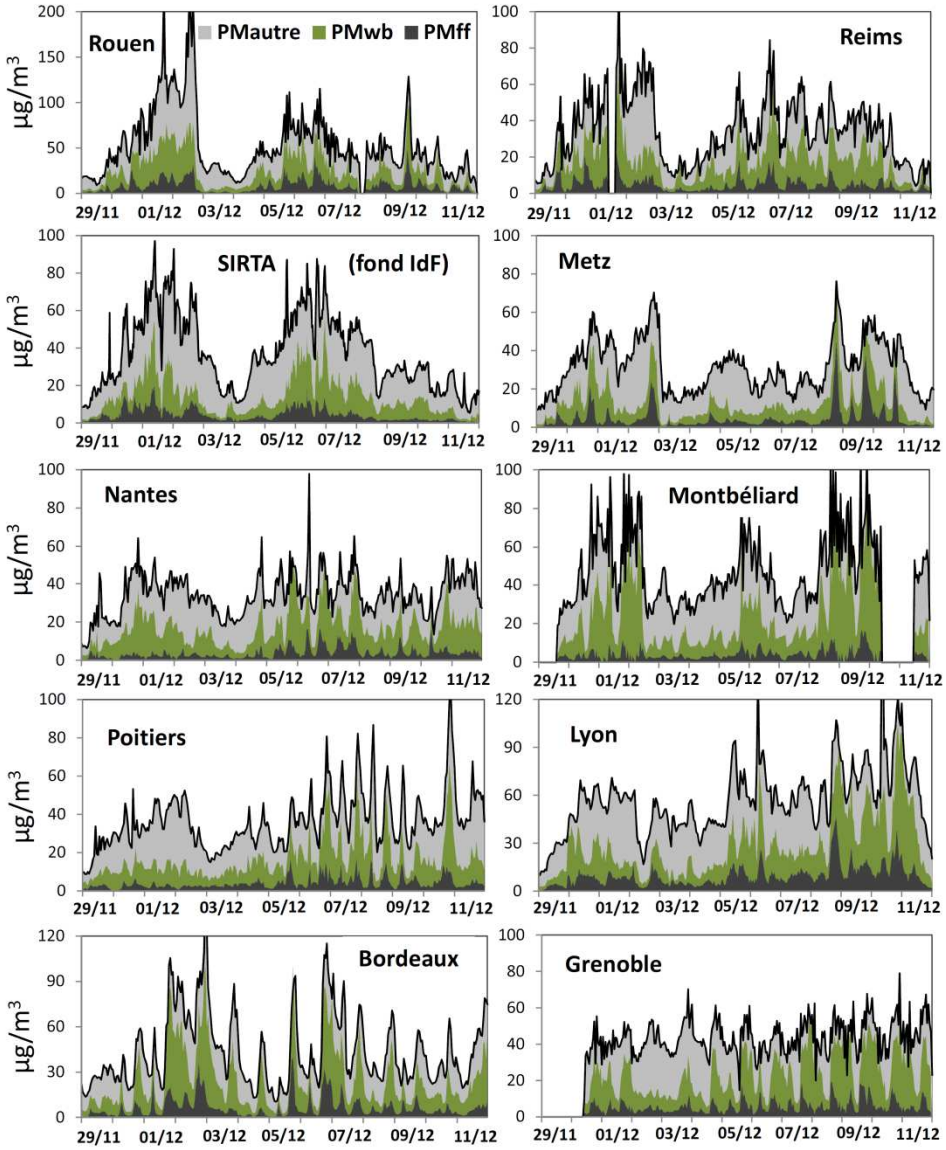

Figure 4 : suivi temporel des concentrations PM_{10} et estimations des fractions issues des émissions primaires liées à la combustion d'hydrocarbures (PM_{ff}) et de biomasse (PM_{wb}) sur différents sites de fond (péri-)urbain entre le 29/11 et le 11/12. (courbes empilées)

2) Couplage avec données ACSM : l'objectif ici est d'estimer la composition des PM_{10} à partir des mesures ACSM et AE33. On évalue d'abord PM_{ff} et PM_{wb} à partir des résultats AE33, comme indiqué précédemment. On reconstruit ensuite les concentrations de nitrate d'ammonium et de sulfate d'ammonium à partir des mesures ACSM de nitrate, de sulfate et d'ammonium et en respectant la stœchiométrie moléculaire. Puis, en considérant que la majeure partie du sulfate d'ammonium, du nitrate d'ammonium et des aérosols organiques secondaires est essentiellement présente au sein de la fraction $PM_{2.5}$, il est possible d'extrapoler les données ACSM (en PM_1) pour déduire une concentration de ces dernières espèces dans la fraction PM_{10}. Pour ce faire, on multiplie les concentrations obtenues par l'ACSM par le ratio $PM_{2.5}/PM_1$. Les concentrations de nitrate d'ammonium et de sulfate d'ammonium dans la fraction PM_{10} sont alors considérées comme égales aux concentrations mesurées par l'ACSM et corrigées de ce ratio. Les aérosols organiques secondaires (AOS), quant-à eux, peuvent être estimés par différence entre la matière organique totale issue des données ACSM corrigées par ce même ratio et l'estimation des contributions organiques

primaires à partir des mesures AE33. La Figure 5 permet d'illustrer les résultats obtenus à l'aide de cette méthodologie pour la station du SIRTA au cours de l'épisode de pollution de décembre 2016.

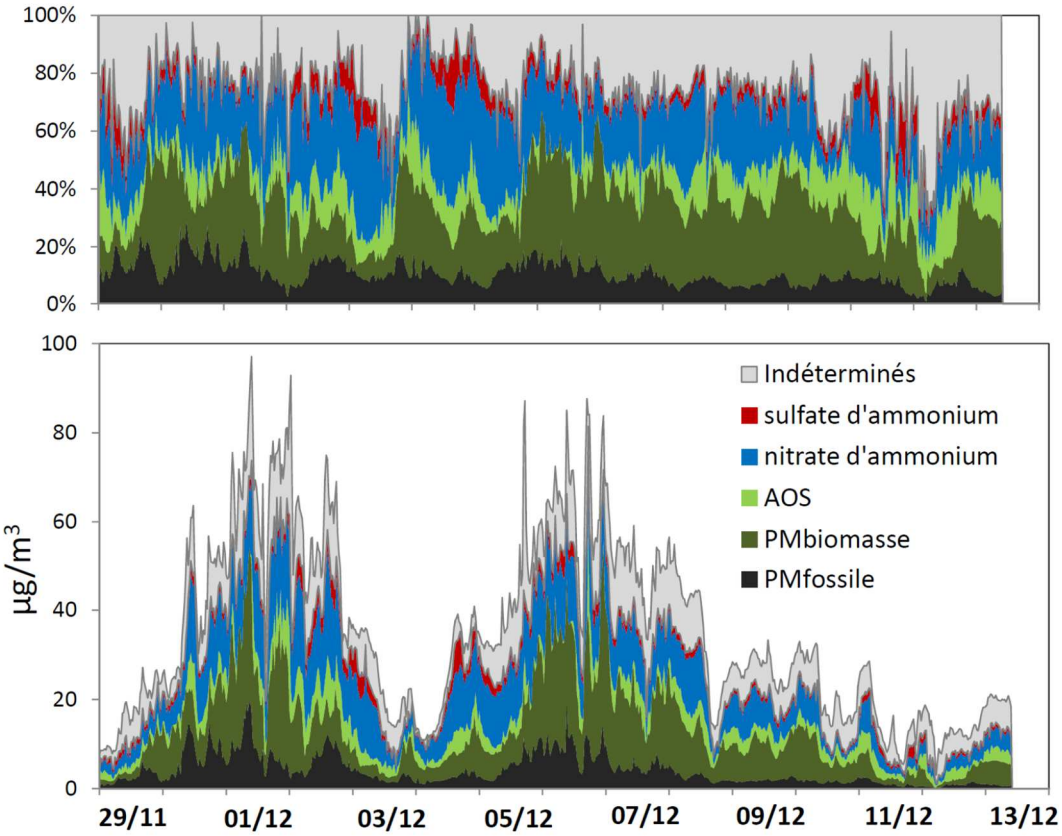

Figure 5 : suivi temporel des concentrations PM_{10} et résultats issus de l'estimation des concentrations de PM_{ff} (PMfossile), PMwb (PMbiomasse), AOS, nitrate d'ammonium et sulfate d'ammonium au SIRTA (courbes empilées)

Cette méthodologie novatrice de traitement de données a notamment été présentée lors de la conférence internationale *Monitoring Ambient Air 2016* organisée à Londres les 12 et 13 décembre 2016 (cf. Annexe 3). Elle correspond à l'état de l'art actuel pour l'exploitation en temps quasi-réel du couplage entre AE33 et ACSM pour l'identification des sources de PM. Une perspective d'optimisation de cette méthodologie est la réalisation d'une analyse préliminaire des sources de la matière organique par analyse PMF automatique des spectres de masses ACSM. Ce travail de développement méthodologique sera réalisé sur la période 2017-2019 en collaboration avec le Paul Scherrer Institute (PSI), laboratoire de recherche suisse leader dans le traitement des données de spectrométrie de masse pour aérosols au sein de la communauté internationale. Une autre voie d'optimisation réside dans le couplage des mesures AE33 et ACSM avec celles issues de la mesure à haute résolution temporelle (e.g., toutes les 2 heures) d'éléments métalliques et metalloïdes caractéristiques de différentes sources d'émission. Différents analyseurs automatiques candidats sont actuellement en cours d'évaluation dans le cadre des travaux du LCSQA pour la mesure des métaux. [20]

6. REFERENCES

[1] Description du programme CARA du dispositif national de surveillance de la qualité de l'air. Note LCSQA 2014. http://www.lcsqa.org/rapport/2014/ineris/description-programme-cara-dispositif-national-surveillance-qualite-air

[2] Méthodologies de détermination de la composition chimique des particules submicroniques en temps réel. Note LCSQA 211. http://www.lcsqa.org/rapport/2011/ineris/note-methodologies-determination-composition-chimique-particules-submicroniques-

[3] Synthèse des travaux 2013 du programme CARA. Rapport LCSQA 2013. http://www.lcsqa.org/rapport/2013/ineris/synthese-travaux-2013-programme-cara

[4] Périmètre de mise en œuvre d'Aerosol Chemical Speciation Monitors (ACSM) pour la mesure automatique de la composition chimique des PM au sein du dispositif national de surveillance de la qualité de l'air. Note LCSQA 2013.
http://www.lcsqa.org/rapport/2013/ineris/perimetre-mise-oeuvre-aerosol-chemical-speciation-monitors-acsm-mesure-automatiq

[5] Point d'étape sur l'implantation des ACSM en AASQA pour les besoins nationaux. Note LCSQA 2016. http://www.lcsqa.org/rapport/2016/ineris/point-etape-implantation-acsm-aasqa-besoins-nationaux

[6] Description des actions menées pour la mise en place des ACSM (Aerosol Chemical Speciation Monitor) au sein du dispositif national de surveillance de la qualité de l'air. Note LCSQA 2015. http://www.lcsqa.org/rapport/2015/ineris/description-actions-menees-mise-place-acsm-aerosol-chemical-speciation-monitor-s

[7] Episodes de pollution particulaire de début Décembre 2016 : Eléments de compréhension à partir des mesures automatiques (période du 30 novembre au 12 décembre 2016), Note LCSQA du 13 Décembre 2016.
http://www.lcsqa.org/rapport/2016/ineris/episodes-pollution-particulaire-debut-decembre-2016-elements-comprehension-par-0

[8] Episodes de pollution particulaire de décembre 2016 : éléments de compréhension à partir des mesures de composition chimique. Rapport LCSQA 2017.
https://www.lcsqa.org/rapport/2017/ineris/episodes-pollution-particulaire-debut-decembre-2016-elements-comprehension-parti

[9] Programmes de recherche expérimentaux pour l'étude des sources de PM en air ambiant. Rapport LCSQA 2016. Ref. INERIS : DRC-16-159637-12364

[10] Synthèse des travaux 2012 du programme CARA. Rapport LCSQA 2012. http://www.lcsqa.org/rapport/2012/ineris/metrologie-particules-pm10-pm25-caracterisation-chimique-particules-synthese-tra

[11] Mise en œuvre d'un « modèle récepteur » de type PMF (« Positive Matrix Factorization ») pour l'identification et la quantification des principales sources de PM_{10} sur le site urbain de fond de Lens (Atmo Nord Pas de Calais). Rapport LCSQA 2012. http://www.lcsqa.org/rapport/2012/ineris/mise-oeuvre-modele-recepteur-type-pmf-positive-matrix-factorization-identificati

[12] LCSQA, 2013b. Mise en œuvre d'une méthodologie d'estimation des sources de HAP par modèle récepteur. Application de la Positive Matrix Factorization (PMF). Rapport LCSQA 2013. http://www.lcsqa.org/rapport/2013/ineris/mise-oeuvre-methodologie-estimation-sources-hap-modele-recepteur-application-pos

[13] Bilan des travaux 2014-2015 du programme CARA. Rapport LCSQA 2015. http://www.lcsqa.org/rapport/2013/ineris/synthese-travaux-2013-programme-cara

[14] European Guide on Air Pollution Source Apportionment with Receptor Models. Belis, C. A., Larsen, B. R., Amato, F., Haddad, I. El, Favez, O., Harrison, R. M., Hopke, P. K., Nava, S., Paatero, P., Prévôt, A., Quass, U., Vecchi, R. and Viana, M.: Publ. Off. [online] Available from: http://source-apportionment.jrc.ec.europa.eu/Docu/EU_guide_on_SA.pdf, 2014

[15] A new methodology to assess the performance and uncertainty of source apportionment models II: The results of two European intercomparison exercises. Belis et al., *Atmospheric Environment*, 123, 240-250, 2015.

[16] Traitement harmonisé de jeux de données multi-sites pour l'étude des sources de PM par Positive Matrix Factorization. Rapport LCSQA 2016. Ref. INERIS : DRC-16-152341-07444

[17] Identification of the main sources and geographical origins of PM10 in the Northern part of France. Manuscrit de thèse de Diogo Oliveira. Thèse de doctorat de l'université de Lille 1 soutenue en janvier 2017. https://www.theses.fr/201433516

[18] Etude de la composition chimique et des sources de particules sur le centre ville de Poitiers. Rapprt d'étude Atmo Nouvelle Aquitaine, 2016.
http://www.atmonouvelleaquitaine.org/sites/aq/files/atoms/files/rapportatmona_fix_int_14_022_caracterisationparticulespoitiers_2015_2016_versionfinale_2017_01_04.pdf

[19] Impact de la combustion de biomasse sur les concentrations de PM10 (programme CARA - hiver 2014-2015). Rapport LCSQA 2015. http://www.lcsqa.org/rapport/2015/ineris/impact-combustion-biomasse-concentrations-pm10-programme-cara-hiver-2014-2015

[20] Evaluation du potentiel technique et scientifique des analyseurs en continu de métaux dans les PM_{10} par fluorescence X. Note LCSQA 2016. https://www.lcsqa.org/rapport/2016/mines-douai/evaluation-potentiel-technique-scientifique-analyseurs-continu-metaux-pm10-

7. LISTE DES ANNEXES

Annexes	titre
Annexe 1	Publication scientifique relative à l'analyse de l'épisode de pollution particulaire de mars 2015 (Petit et al., *Atmospheric Environment*, 155, 68-84, 2017).
Annexe 2	Description des sites et méthodologies de spéciation chimique utilisés pour l'obtention des jeux de données étudiés dans le cadre de l'analyse PMF harmonisée du projet SOURCES.
Annexe 3	Présentation du programme CARA lors de la conférence *Monitoring Ambient Air* 2016 (Londres, 12-13 décembre 2016).

Publication scientifique relative à l'analyse de l'épisode de pollution particulaire de mars 2015.

Petit et al., *Atmospheric Environment*, 155, 68-84, 2017.

Characterising an intense PM pollution episode in March 2015 in France from multi-site approach and near real time data: climatology, variabilities, geographical origins and model evaluation.

J.-E. Petit[1], T. Amodeo[2], F. Meleux[2], B. Bessagnet[2], L. Menut[3], D. Grenier[4], Y. Pellan[4], A. Ockler[1], B. Rocq[5], V. Gros[6], J. Sciare[6, 7], O. Favez[2]

[1]Air Lorraine, 20 rue Pierre Simon de Laplace, 57070 Metz, France

[2]INERIS, rue Jacques Taffanel, 60750 Verneuil-en-Halatte, France

[3]Laboratoire de Météorologie Dynamique, Palaiseau, France

[4]Air Rhône-Alpes, 3 allée des Sorbiers, 69500 Bron, France

[5]Atmo Picardie, 22 boulevard Michel Strogoff, 80332 Longueau, France

[6]Laboratoire des Sciences du Climat et de l'Environnement, CEA/Orme des Merisiers, 91191 Gif-sur-Yvette, France

[7]The Cyprus Institute, Energy Environment Water Research Center, Nicosia, Cyprus

Correspondence to: J.-E. Petit (jean-eudes.petit@atmo-grandest.eu) & O. Favez (olivier.favez@ineris.fr)

Keywords: aerosol, pollution, France, Aerosol Chemical Speciation Monitor, ACSM, Aethalometer, model

Abstract

During March 2015, a severe and large-scale particulate matter (PM) pollution episode occurred in France. Measurements in near real-time of the major chemical composition at four different urban background sites across the country (Paris, Creil, Metz and Lyon) allowed the investigation of spatiotemporal variabilities during this episode. A climatology approach showed that all sites experienced clear unusual rain shortage, a pattern that is also found on a longer timescale, highlighting the role of synoptic conditions over Wester-Europe. This episode is characterized by a strong predominance of secondary pollution, and more particularly of ammonium nitrate, which accounted for more than 50% of submicron aerosols at all sites during the most intense period of the episode. Pollution advection is illustrated by similar variabilities in Paris and Creil (distant of around 100 km), as well as trajectory analyses applied on nitrate and sulphate. Local sources, especially wood burning, are however found to contribute to local/regional sub-episodes, notably in Metz. Finally, simulated concentrations from Chemistry-Transport model CHIMERE were compared to observed ones. Results highlighted different patterns depending on the chemical components and the measuring site, reinforcing the need of such exercises over other pollution episodes and sites.

1. Introduction

Particulate pollution is nowadays subject to extensive studies notably due to particulate concentrations that exceed the recommended limits and demonstrated health effects on a short- and long-term perspective (Ramgolam et al., 2009; IARC, 2013). Also, increasing population density within urban areas tends to enhance the exposure to pollution. Worldwide, frequent PM pollution episodes occur, where the North-China Plain (e.g. Zhang et al., 2015) and the Indo-Gigantic Plain (e.g. Chakraborty et al., 2015) experience the most severe and intense ones. In China, for example, Huang et al., 2014) have recently highlighted strong specificities (i.e. spatial variability) in urban areas, in terms of chemical composition, and also sources, even if the overall aerosol burden is dominated by secondary material. France, as well as Western-Europe, is frequently subject to large-scale PM pollution episodes, notably during winter and spring (Bessagnet et al., 2005; Sciare et al., 2010; Favez et al., 2012; Bressi et al., 2013; Waked et al., 2014; Rouïl et al., 2015). Paris region being the most densely inhabited region in France, and has benefited over the years from extensive studies on the chemical characterization of the particulate phase in order to better understand the sources and the formation of aerosol pollution. Intensive campaigns and 1-year daily filter sampling have highlighted the predominance of ammonium nitrate during pollution episodes, and strongly influenced by long-range transported pollution (70% on average of PM pollution is thought to originate outside of the Paris region), pointing to large scale episodes in North-Western Europe dominated by secondary pollution (Beekmann et al., 2015), which has been also supported from mobile (von der Weiden-Reinmüller et al., 2014) and aircraft (Freney et al., 2014) measurements over the region during winter and summer. Long-term measurements in near real time between mid-2011 and mid-2013 have emphasized episode-to-episode variability, where significant discrepancies were observed in terms of sources, meteorological conditions, geographical origins and (trans-)formation processes (Petit et al., 2015), concluding that each episode was actually representative of itself only.

However, if global homogeneity is found over the Paris region, little is known about spatial variability at a bigger geographical scale than the Ile-de-France region, although significant discrepancies have already been observed at the national scale from filter measurements (Favez et al., 2012; Rouïl et al., 2015). Due to poor temporal resolution, these measurements cannot unfortunately describe the diurnal evolution of the chemical composition. Moreover, Chemistry-Transport Model (CTM) evaluation has been extensively performed for the Paris region, but is poorly documented in other French urban areas. Since meteorology and sources may differs from a pollution episode to another, and from site to site, model performance should vary accordingly. Therefore, spatial variability represents very important information although rarely addressed during pollution episodes. The main limitation of investigating this variability is related to the capability of deploying state-of-the-art instrumentation over several sites across the country.

Since early 2015, real-time measurements of the major chemical composition of submicron aerosols have been performed in other cities than Paris within regional air quality networks, with Aerosol Chemical Speciation Monitor (ACSM, Ng et al., 2011) and 7-wavelength Aethalometer (AE33, Drinovec et al., 2013). These two instruments have been proven to be very robust over long-term periods (Herich et al., 2011; Petit et al., 2015), and are adequate tools to document temporal variabilities on a refined timescale.

This article aims to describe a severe PM pollution episode that occurred in France during March 2015. Climatology, spatiotemporal variabilities, geographical origins and a model evaluation are presented in the following sections.

2. Material and methods

2.1 Sites description

Figure 1 shows the location of the 4 different measuring sites used in this study; detailed geographical coordinates are summarized in Table 1. Located 20 km South-West of Paris, the SIRTA atmospheric supersite is a multi-instrumented structure for the long-term physical and chemical characterization of the troposphere in the Paris region (Haeffelin et al., 2005). In-situ measurements of aerosols have continuously been performing there since mid-June 2011 (Petit et al., 2015). The 3 other stations, in Creil, Metz and Lyon are part of their respective regional air quality network, namely Atmo Picardie (http://www.atmo-picardie.com), Air Lorraine (http://www.air-lorraine.org) and Air Rhône-Alpes respectively (http://air-rhonesalpes.fr). These stations are representative of urban background air quality. The chemical characterization of submicron aerosols has been continuously performed in Lyon and Metz since early 2015, while in Creil a specific instrumentation has been deployed only from February to April 2015.

Figure 1: Location of the 4 stations used in this study. Black: SIRTA; blue: Creil; red: Metz; purple: Lyon

Table 1: Coordinates and typology of the 4 different sites

	Longitude (°)	Latitude (°)	Background
SIRTA	48.71	2.15	Regional/semi-urban
Creil	49.26	2.47	Urban
Metz	49.11	6.22	Urban
Lyon	45.76	4.85	Urban

2.2 Instrumentation

Recently developed, the Aerosol Chemical Speciation Monitor (Aerodyne Research Inc., Ng et al., 2011a) offers the measurements of the major chemical composition of non-refractory submicron aerosols. Concentrations of organic matter (OM), nitrate (NO_3^-), sulphate (SO_4^{2-}), ammonium (NH_4^+) and chloride (Cl^-) are determined at time resolution around 30 min. Briefly, particles are sampled at 3 L/min, and sub-sampled at 0.1 L/min through a focusing lens allowing a submicron aerosol beam to be focused on a 600°C-heated vaporizer. Particles are flash-vaporized, and quasi-instantaneously ionized and fragmented by electron impact at 70 eV. Produced fragments are separated by a quadrupole analyser before their detection; a fragmentation panel (Allan et al., 2004) eventually allows the calculation of chemical species following their fragmentation patterns.

The determination of the response factor of the ACSM is performed by injecting generated 300 nm ammonium nitrate particles into the ACSM and a Condensation Particle Counter (CPC). The full procedure is available in Ng et al. (2011a). Table 2 summarizes the response factors and relative ion efficiencies (RIE) used for the different ACSMs. As ammonium sulphate calibration is still subject to investigation, it was decided here, for consistency, to apply a default RIE_{SO4} of 1.2 for all ACSMs. This is however confirmed by an overall neutrality of secondary inorganic aerosols, observed for all sites.

Table 2: Response factors and RIEs used for the 4 ACSMs

	Response factor (10^{-11}A/µg/m^3)	RIE_{NH4}	RIE_{SO4}
SIRTA	4.22	5.25	1.2
Creil	4.32	6.18	1.2
Metz	2.06	8.00	1.2
Lyon	5.34	6.41	1.2

Collection efficiencies (CE) have been corrected following the ammonium nitrate mass fraction by the algorithm proposed in Middlebrook et al. (2012). An additional CE correction has been applied in Metz between 05/03 and 11/03 following the recommendation of Alfarra et al. (2007), where a fixed CE of 0.7 was used during a wood-burning-dominated episode.

Finally, intercomparability between the chemical species measured by ACSMs is ensured from a recent intercomparison exercise that assessed satisfying reproducibility for OM, NO_3^-, SO_4^{2-} and NH_4^+ (Crenn et al., 2015). Extended uncertainty of 15, 19, 28 and 36% has respectively been calculated for these species. Although more significant discrepancies are observed for mass fragments (and notably m/z 44), this paper focuses on the variability of the chemical components; the interpretation is thus not subject to those uncertainties.

Absorption measurements were performed by 7-wavelength aethalometers (AE33, Magee Scientific). The AE33 model specifically uses a Dual-Spot technology enabling the automatic compensation of the loading effect (Drinovec et al., 2015) over the 7 wavelengths, from near UV to near IR. 1-min Black Carbon (BC) data (at any wavelength) below or equal to 0, or associated with an Angstrom exponent (calculated from the 7 wavelengths, and not two as traditionally performed) below 0.75 or above 3, or regression coefficient (r^2) below 0.9, were discarded. Possibly due to high scattering, which is not corrected within the AE33, during the pollution episode linked to high ammonium nitrate concentrations, loss of automatic compensation has been observed at SIRTA and Metz during several days. The associated data were thus manually re-compensated with fixed k values empirically determined to minimize the jumps between spot changes. Table 3 lists the k combinations used for the 2 different sites.

Table 3: manually-determined compensation parameters k at SIRTA and Metz

	period	k_1	k_2	k_3	k_4	k_5	k_6	k_7
SIRTA	14/03 – 21/03	0.0058	0.0061	0.00625	0.0064	0.00655	0.0069	0.007
METZ	18/03 - 21/03	0.0041	0.00419	0.00439	0.0044	0.00443	0.00426	0.00434

BC concentrations were apportioned in Paris, Lyon and Metz, taking advantage of the multi-wavelength measurement of the AE33. Assuming that biomass burning and fossil fuel combustion are the two predominant sources of BC, and that the first cited is mostly responsible of the enhanced absorption observed at near-UV wavelengths, the contribution of the two sources to BC can be deconvolved (see Sandradewi et al., 2008). Although some

limitations of this methodology have been observed in India (Garg et al., 2015), it has already been successfully applied in Paris (Sciare et al., 2011; Petit et al., 2014) as well as other cities in France (Favez et al., 2010) and elsewhere (Herich et al., 2011; Briggs and Long, 2016).

One source of uncertainties in this approach is the choice of the Angstrom absorption exponents of fossil fuel and biomass burning (α_{ff} and α_{wb}, respectively) that may vary from site to site. Here, these two parameters were determined at each site from the diurnal distribution of the Angstrom exponent. Then, a sensitivity test was performed by documenting the impact of small changes in α_{wb} and α_{ff} by varying the initial values by ± 0.05 with a step of 0.01. The optimized exponents are found for a minimum number of BC_{ff}<0 (i.e. BC_{wb} > BC) (Table 4). It is to note that these small variations of exponents (α ± 0.05) don't lead to significant discrepancies in terms of concentrations, except for low values (< 0.5 µg/m^3). The α_{wb} values listed in Table 4 significantly differ from a recent study which recommends 1.68 as more suitable value (Zotter et al., 2016). However, at SIRTA for example, applying this coefficient leads to much higher BC_{wb} concentrations (+ 115% on average) compared to the decrease of BC_{ff} (-31% on average), and thus to a higher occurrence of (BC_{ff} + BC_{wb}) > BC.

Table 4: Absorption exponents used at each site for wood burning (wb) and traffic (ff)

	α_{wb}	α_{ff}
SIRTA	2	1
Metz	1.95	1
Lyon	1.85	1.05

Urban background PM_{10} and $PM_{2.5}$ concentrations were provided at SIRTA from TEOM-FDMS (Tapered Element Oscillating Microbalance – Filter Dynamics Measurement System) and in Creil, Metz and Lyon from BAM (Beta Attenuation Monitoring) instrument. Note that, for Metz, co-located particle mass measurements at only PM_{10} were available at the station. This is why PM_{10} and $PM_{2.5}$ concentrations were retrieved from another urban background station located 5 km away. Comparison of PM_{10} at both sites shows excellent consistency, with slope of 1.02 and r^2 of 0.79, for 1-h averages from 01/01/2015 to 18/08/2015.

The instrumentation used in this study are summarized in Table 5.

Table 5: Summary of instruments used in this study at each site.

	SIRTA	CREIL	LYON	METZ
PM_1 NR chemical composition (ACSM)	√	√	√	√
Black Carbon (AE33)	√		√	√
$PM_{2.5}$ (TEOM-FDMS)	√	√	√	√*
PM_{10} (TEOM-FDMS)	√	√	√	√* (BAM)

*As described above, PM concentrations in Metz were retrieved from BAM measurements from another urban background station.

2.3. Cluster and Concentration-Weighted Trajectory

Since wind direction measured at punctual site is not necessarily representative of the supra-regional origin of the air mass, backtrajectories were calculated every 3 hours at the 4 measuring stations using the PC-based version of HYSPLIT v4.1 (Draxler, 1999; Stein et al., 2015), using the ending (lon, lat) couples listed in Table 1, and an ending altitude of 100 m

above ground level (a.g.l.). Weekly Global Data Assimilation System (GDAS) files with a 1° resolution were used. Cluster analysis was subsequently applied to the obtained backtrajectories, and allowed the gathering in more general geographical origin. The optimal number of clusters was assessed from the total spatial variance (TSV) variation (Elbow approach). 6, 9, 7 and 7 clusters were respectively used at SIRTA, Creil, Metz and Lyon. Their mean trajectories are represented in Figure 2.

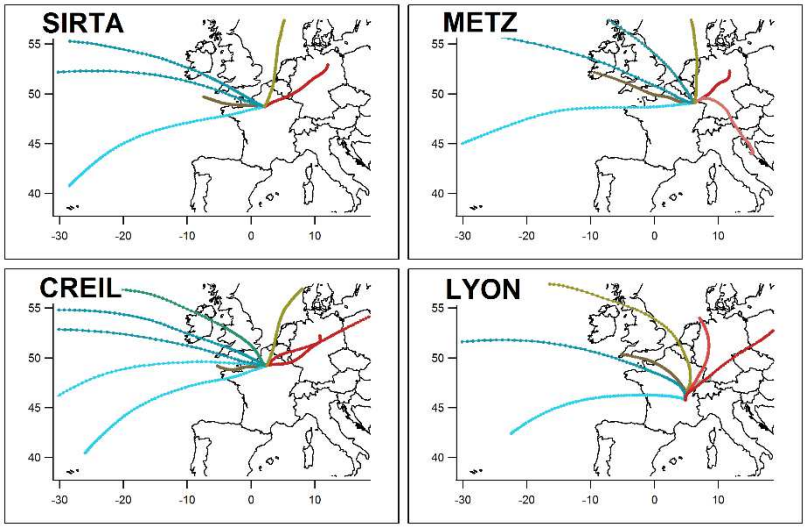

Figure 2: Mean Trajectories for each cluster at all measuring sites. The colour of each cluster represents its global geographical origin, and is consistent throughout this paper.

More precise geographical origin work has also been performed by Concentration-Weighted Trajectory (CWT). This approach couples concentration data measured at a receptor site with backtrajectories and helps to localize air parcels responsible for high measured concentrations at the receptor site (Ashbaugh et al., 1985). CWT values is computed by:

$$\overline{C}_{ij} = \frac{\sum_l^N C_l \cdot \tau_{ijl}}{\tau_{ijl}},$$

Where C_{ij} is the estimated concentration in each ijth air parcel, C_l the concentration measured at t_l, N the total number of concentration values, and τ_{ijl} the residence time (in hour) in each ijth cell of trajectory arriving at the receptor site at t_l. In order to match the time resolution of backtrajectories, all concentrations were averaged upon a 3-h basis. Similarly to Waked et al. (2013) and Bressi et al. (2014) for Potential Source Concentration Function (PSCF) calculations, precipitation data have been calculated along trajectories and have been used to remove endpoints after rain occurred. Endpoints at altitudes above 3000 m a.g.l. were also discarded.

Trajectory-based approaches conceptually fails to provide meaningful information for pollutants that can have local/regional contributions. Removing these signals is particularly difficult without comprehensive source apportionment, but is essential to prevent additional noise in the analysis. Here, wind speed values were used to discriminate periods when only local/regional emissions occur. We empirically chose the 10th percentile value of the wind speed at each site to create a sub-set, where only local/regional pollution is present. The choice of a variable threshold depending on the site is mainly justified by different dispersion conditions, linked to the surrounding geomorphologies (e.g. see the average wind roses Figure S1). This does not prevent from local contributions in the analysis, but does remove the periods where no advection occurs.

Calculations and graphing have been performed on Igor© with ZeFir, an Igor package for the

evaluation of the geographical origins of atmospheric pollution (Petit et al., submitted).

2.4. Chemical composition from Chemical Transport Model (CTM)

The chemistry transport model used here to retrieve the chemical composition of submicron aerosols is CHIMERE, largely used through Prev'air (http://www.prevair.org), the national platform of air quality forecasting. The details of the different modules used in CHIMERE can be found in Menut et al. (2013). Briefly, chemical mechanisms are modelled through MELCHIOR (Lattuati, 1997), thermodynamic partitioning is computed from ISORROPIA model (Nenes et al., 1998), meteorological parameters are retrieved from global GFS data, and refined with MM5 input. Finally, gaseous and particulate emissions are derived from EMEP annual totals, and downscaled from land-use data for spatially-refined data.

Simulated NO_3, SO_4, OM, BC, ambient temperature and relative humidity at D+1 are presented in this study. Normalized Mean Bias (NMB) between measured and modelled concentrations are calculated as:

$$NMB = \frac{1}{N}\frac{\sum_i^N (m_i - o_i)}{\bar{o}}$$

where m_i, o_i, N and $\bar{o}$ respectively represent modeled and observed concentrations, number of points, and average observed concentration.

3. Results & Discussions

3.1. Climatology

Monthly averaged meteorological parameters (temperature, accumulated rainfall and hours of sunshine) were compared, at all sites, with their monthly normal values at that period of the year. Results are illustrated in Figure 3. Although the four sites are subject to a different climatology (except Creil and SIRTA which are relatively close to each other), the striking feature is a clear rainfall shortage at all sites, from -13% in Lyon to -44% in Creil. This was also observed in the region of Paris during high PM polluted episodes in March 2012 and 2013 (Petit et al., 2015), as well as during the pollution episode of March 2014 described in Dupont et al. (2016). Indeed, low rainfalls reduce the removal of particles by wet deposition and enhance their persistence within the atmosphere. Moreover, rainfalls were essentially concentrated at the beginning and at the end of the month, letting around 20 dry days at all sites. Consequently, March 2015 was more sunny than usual, except in Lyon, which shows a slight shortage close to normal. Thus, temperature does not appear here to be the key meteorological parameter that controls the formation of this pollution episode, but could however drive the diurnal temporal variability of certain species, notably regarding semi-volatile aerosols. This feature is observed over a wider geographical scale, as Western Europe experienced precipitation shortage, especially Northern France, the Netherlands, Belgium, Luxemburg, Western Germany and Southern United Kingdom (UK) (Figure S2a). Large-scale precipitation patterns can be linked to synoptic atmospheric circulation (Jones and Lister, 2009). Indeed, March 2015 is associated with a positive sea-level pressure anomalies (Figure S2b), between 4 and 6 hPa over these regions, and Lavers et al. (2013) have shown the relationships between pressure fields and precipitation at the European scale.

This trend is also observed on a much longer perspective when correlating PM_{10} and precipitation difference to normal from 2007 to 2015 (Fig. 4). Normal precipitation values were not available in Creil, but given i) the relative proximity to Paris and ii) the rather flat orography in this area of the Parisian Basin, we hypothesize that results in Creil can be somewhat similar to what is observed in Paris. Monthly PM_{10} 'normal' values were calculated from monthly averages between 2007 and 2015; due to the implementation within monitoring networks of FDMS measurements in 2007, any prior concentrations are not fully comparable. It globally appeared that the highest PM_{10} to normal positive differences (from 8 to higher than 25 µg/m^3) occurred at the highest PM_{10} concentrations, and are associated with unusual rain shortage. Interestingly, these extreme events are observed mostly during spring, except in Lyon where they are more associated to winter months; suggesting thus different sources and/or atmospheric processes involved. Then, March 2015 in Lyon and Paris is not unusually more polluted, with differences to normal that are close to 0 (around 3 µg/m^3 in absolute value), whereas in Metz appears to be, with +8.4 µg/m^3 of PM_{10} difference, among the most heavy-polluted months since January 2007.

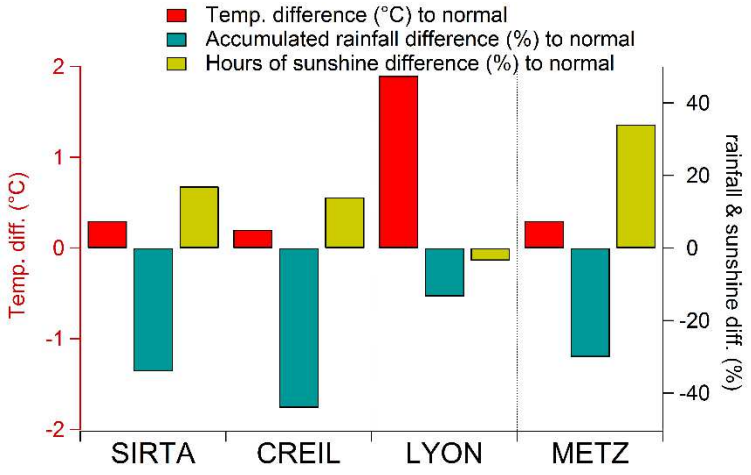

Figure 3: Differences to normal values (calculated over a 30-year period) for different meteorological parameters (temperature, rainfall amount and hours of sunshine) at all sites during March 2015.

Long term scenario simulations report that precipitation, more than temperature, controls the evolution of $PM_{2.5}$ concentrations (e.g. Jacob and Winner, 2009; Dawson et al., 2009; Peel et al., 2013). Indeed, it is found that increasing precipitation frequency leads to decreasing $PM_{2.5}$. Our results, based on surface measurements, meet their conclusions from another angle: most intense pollution episodes are mostly associated with unusually dry conditions. Recent climatological studies linked haze pollution episodes in China with autumnal Artic ice melting (Wang and Chen, 2016), or synoptic weather patterns (Zhang et al., 2016). In Europe, it has been proven that atmospheric circulation has been the root of an unusually wet month of June 2012 in Western Europe (Yiou and Cattiaux, 2013). On the other hand, atmospheric circulation favouring dry conditions during spring could enhance a risk of pollution events. Moreover, climatic predictions for France report a slight decrease of precipitation in Northern France (Habets et al., 2013), and an increase of dry spells depending on the scenario (Kovats et al., 2014), leading again to an increased risk of springtime PM pollution episodes due to unfavourable meteorological conditions. Pausata et al. (2013) have concluded that the North-Atlantic Oscillation Index (NAOI) can be a useful tracer of the impact of the change of

atmospheric circulation linked with PM pollution. Indeed, variations of precipitation patterns control the evolution of aerosol concentrations, being thus linked to changes of NAO phases (Pokrovsky, 2009; Jerez et al., 2013). However, in our case and applied to our dataset, no clear connection between NAOI and PM anomalies or rainfall anomalies were found (Figure S3). A more comprehensive study, including weather regimes with additional sites may provide more precise outcomes, similarly to (Pope et al., 2015) on NO_x data over UK.

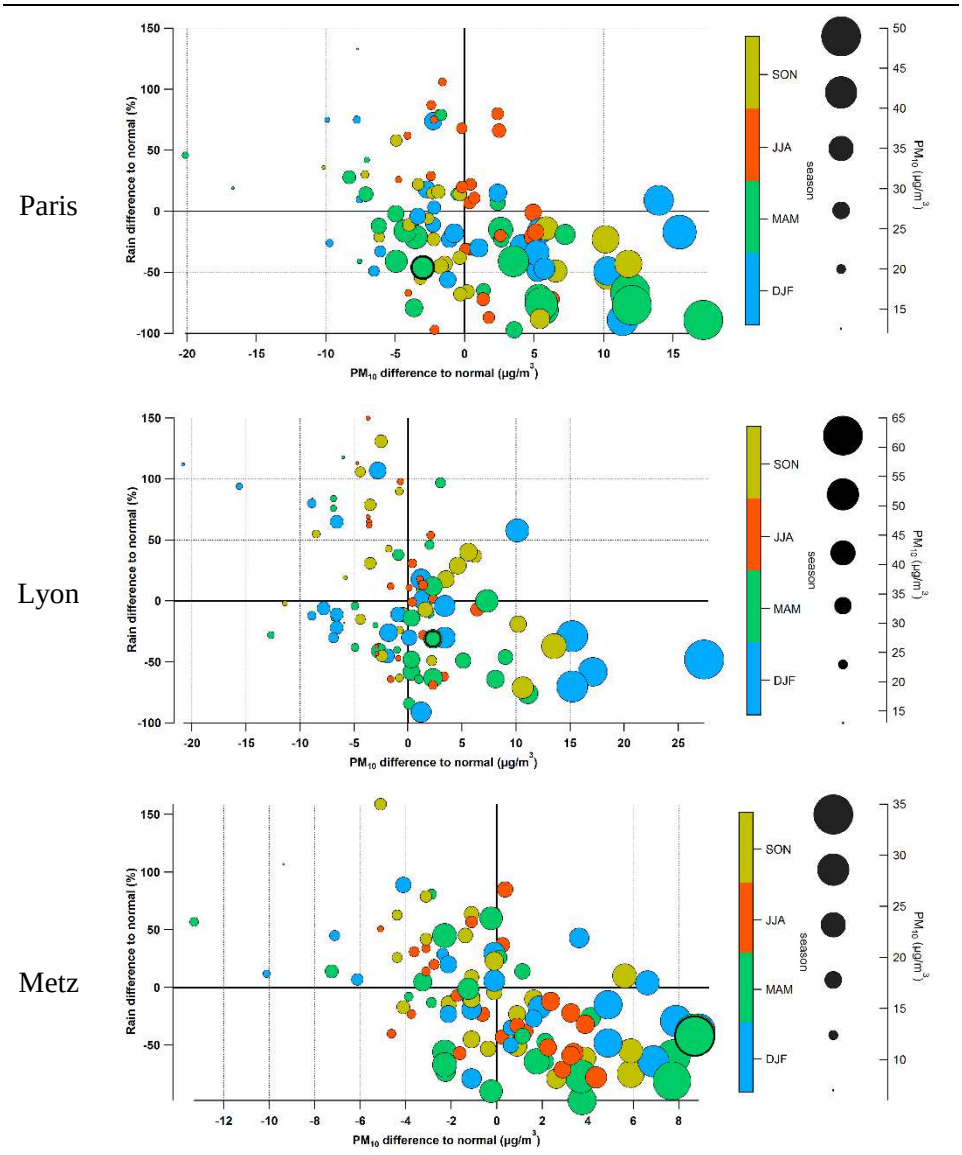

Figure 4: Monthly PM_{10} and precipitation differences to normal from January 2007 to September 2015. Colour of marker corresponds to the month of the year, size of the marker to the average PM_{10} concentrations (in $\mu g/m^3$). The month of March 2015 has a thicker stroke. Mind the differences in X-axes and markers' size scale.

3.2. Spatial variability

The box and whiskers plot in Figure 5 illustrates the statistical distribution of the chemical composition retrieved from ACSM and AE33 instruments, where arithmetic mean and maximum, p_{10}, p_{25}, p_{50}, p_{75} and p_{90} values were calculated. There absolute values are listed in Table 6.

Table 6: mean, maximum, 10^{th}, 25^{th}, 50^{th}, 75^{th}, and 90^{th} percentiles for each chemical component at all sites.

		mean	max	p_{10}	p_{25}	p_{50}	p_{75}	p_{90}
OM	SIRTA	6.2	28.9	0.9	2.1	5.4	9.1	12.9
	Creil	6.9	40.5	1.2	2.6	5.8	9.6	15.1
	Lyon	5.9	30	1.9	2.9	4.5	7.6	12.1
	Metz	9.5	59.8	1.5	3.4	8.1	13.8	22.1
NO_3	SIRTA	6.6	54.9	0.2	0.9	5.3	9.2	14.3
	Creil	6.5	51.7	0.2	0.9	4.1	8.4	14.5
	Lyon	4.1	34	0.3	0.6	1.7	5	10.5
	Metz	7.7	31.4	0.4	1.7	6	11.6	17.5
SO_4	SIRTA	1.1	8.2	0.1	0.3	0.7	1.5	2.6
	Creil	1.4	15.6	0.3	0.5	1.1	1.9	3.1
	Lyon	0.9	7.9	0.2	0.4	0.6	1	1.5
	Metz	2.6	6.9	0.3	0.6	1.1	2.2	3.6
NH_4	SIRTA	2.1	14.3	0.1	0.4	1.6	2.9	4.9
	Creil	2.1	12.6	0.2	0.6	1.7	3	4.6
	Lyon	1.3	11.6	0.1	0.3	0.7	1.5	3.2
	Metz	1.6	10.6	0.3	0.7	2.2	3.7	5.4
Cl	SIRTA	0.1	0.7	0	0	0.1	0.2	0.3
	Creil	0.4	8.5	0.1	0.2	0.3	0.5	0.9
	Lyon	0.1	4.1	0	0	0.1	0.1	0.2
	Metz	0.2	5.8	0	0.1	0.2	0.3	0.4
BC_{ff}	SIRTA	0.6	4.2	0.1	0.1	0.3	0.7	1.2
	Creil	-	-	-	-	-	-	-
	Lyon	1.4	10.6	0.3	0.6	1	1.7	3.1
	Metz	1.8	4.7	0.2	0.4	0.9	1.6	2.7
BC_{wb}	SIRTA	0.2	1.3	0	0.1	0.2		0.5
	Creil	-	-	-	-	-	-	-
	Lyon	0.3	2	0.1	0.1	0.2		0.6
	Metz	0.5	17.3	0.1	0.2	0.3		0.9

Metz exhibits the highest medians for the major chemical components (OM, NO_3, SO_4 and NH_4), and the highest InterQuartile Range ($IQR=p_{75}-p_{25}$) for the latter species (respectively 10.38, 9.96, 1.61, and 3 $\mu g/m^3$), indicating very pronounced variability in terms of concentrations. Moreover, highest maximum values of OM and BC_{wb} are also found in Metz; wood burning may thus be a strong pollution source in this area of France. It is however in Creil and at SIRTA that highest maximum nitrate concentrations are observed (59.4 and 51.7 $\mu g/m^3$, respectively).

Creil and SIRTA show a very similar distribution with comparable median values for all species (except chloride that is found much higher in Creil due to close-by industrial activities). But given the fact that Creil is located around 100 km NNE of SIRTA and that measurements at SIRTA are more representative of regional background pollution, this can be

whether due to i) homogeneous concentrations over very large scale and similar meteorological conditions, and/or ii) regionally formed ammonium nitrate in the IdF area to compensate atmospheric dilution.

BC_{ff} distribution is narrower in SIRTA than in Lyon and Metz, but as mentioned above, SIRTA is less exposed to high urban traffic and is more representative of regional concentrations for BC when compared to BC measurements downtown Paris (Petit, 2014).

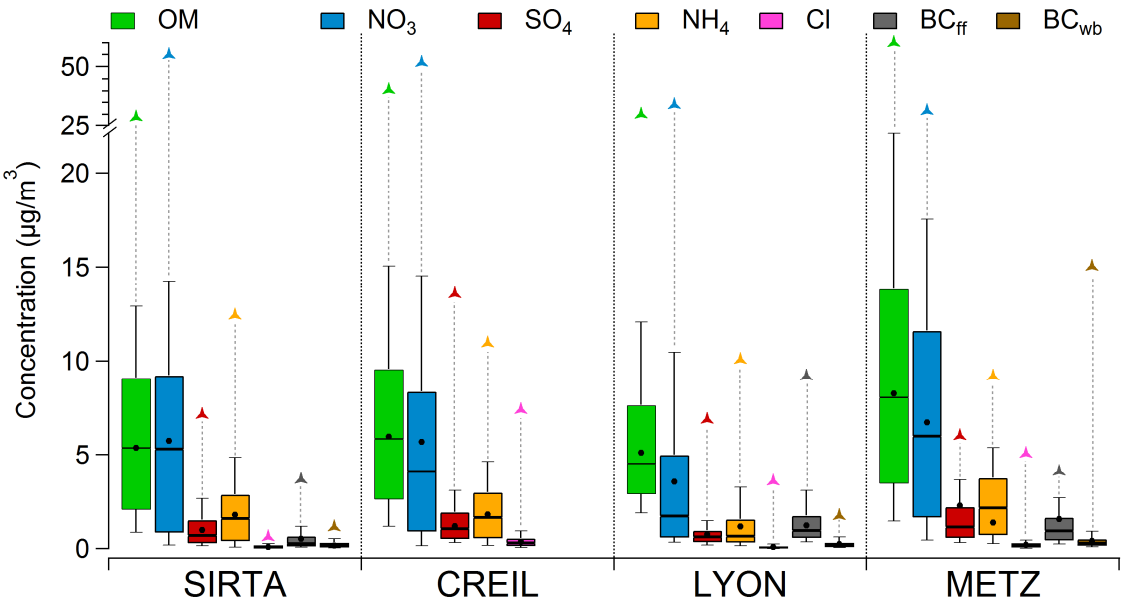

Figure 5: Statistical distribution of the chemical composition at 4 sites. 10th, 25th, 50th, 75th, and 90th percentiles were used. Black dots and coloured arrows respectively correspond to the arithmetic mean and maximum values.

3.3. Temporal variability

Temporal variability of the chemical composition of submicron aerosols at all sites is presented in Figure 6. Additionally, the origin of the air mass is illustrated in the background, where each 3-h bin colour corresponds to one cluster, as defined in Fig. 2. Average composition by cluster at each site is presented in Figure S6. All sites exhibit the highest PM_1 concentrations between March 18th and 21st. The average chemical composition during this period shows with a clear predominance of secondary inorganic aerosols (between 60.8 and 71.2% of PM_1), and notably ammonium nitrate, at all sites. This meets previous observations in Western Europe during pollution episode (Putaud et al., 2010; Petit et al., 2015; Beekmann et al., 2015), but also in Asia (Huang et al., 2014) or in United States (e.g. Kim et al., 2010). However, in Metz, high PM_1 concentrations are also observed between March 7th and 11th, dominated by organic matter (20 µg/m^3 in average, representing 45.9% of PM_1). Significant amount of BC were also found (4.6 µg/m^3 on average during this period, with a maximum 30-min value of 21.6 µg/m^3), with maximum daily amplitude of 20 µg/m^3, which has been rarely seen in urban background in Europe.

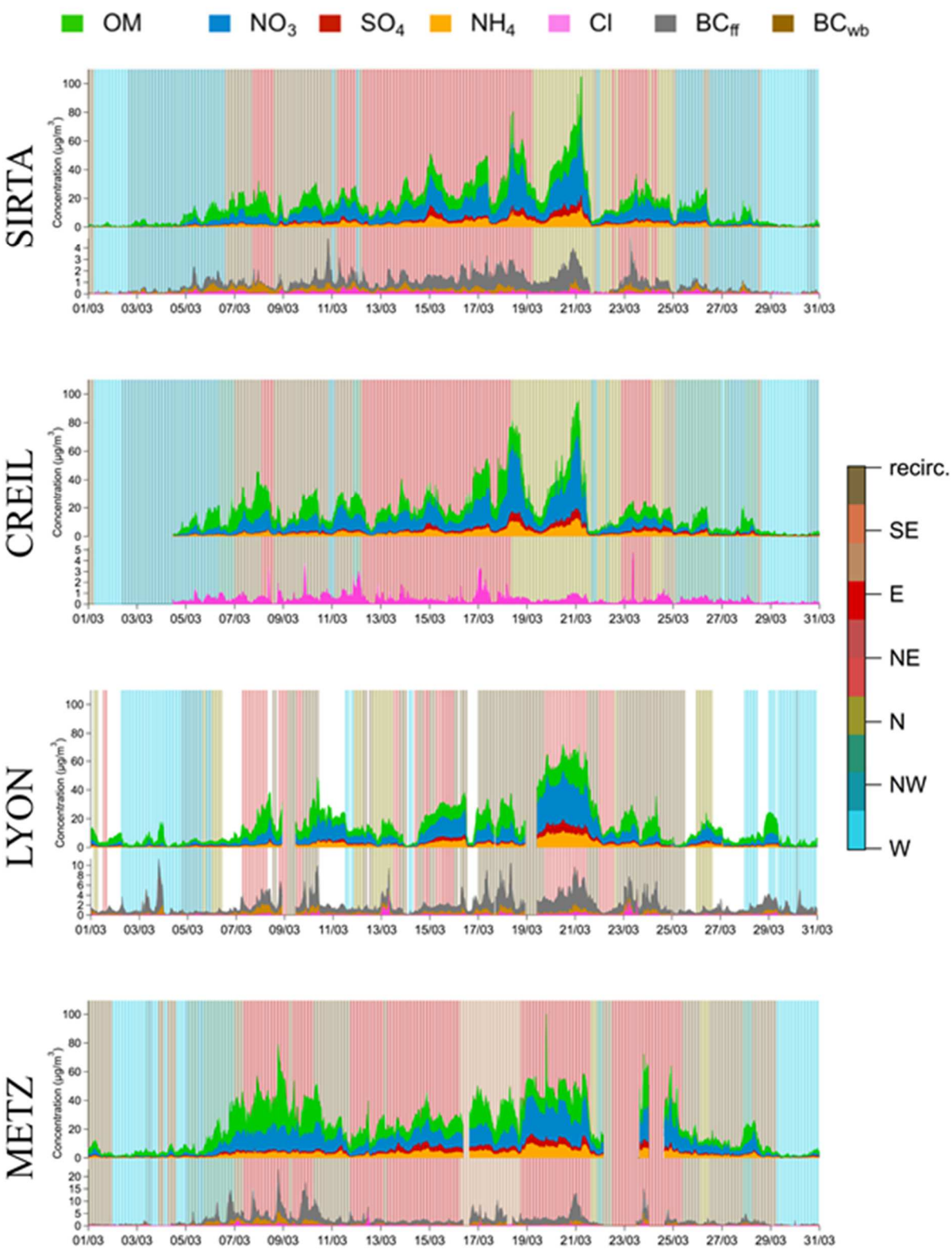

Figure 6: Temporal variability of the chemical composition measured in SIRTA, Creil, Lyon and Metz. Mind the different scales for BC. Background colours refer to air mass clusters, defined in Section 2.

In details, BC_{ff} makes the majority of BC on average during this period (75%), which is consistent with what is regularly observed, meaning that traffic is still a major source of BC.

But BC_{wb} went up to 4.7 µg/m^3, emphasizing the role of local/regional emissions such as wood burning. Fresh wood-burning-related concentrations is supported by distribution of the fraction of m/z60 (denoted f_{60}) and m/z44 (f_{44}) (Cubison et al., 2011). Indeed, m/z60, related to the $C_2H_4O_2^+$ ion (Schneider et al., 2006; Alfarra et al., 2007), is usually used as a key tracer of Biomass Burning Organic Aerosol (BBOA), while m/z44 can be a surrogate of Secondary Organic Aerosol (SOA). This period is characterized by significantly lower f_{44} and higher f_{60} than the rest of the dataset (Figure 7), which is characteristic of fresh wood-burning emissions (Cubison et al., 2011; Ortega et al., 2013).

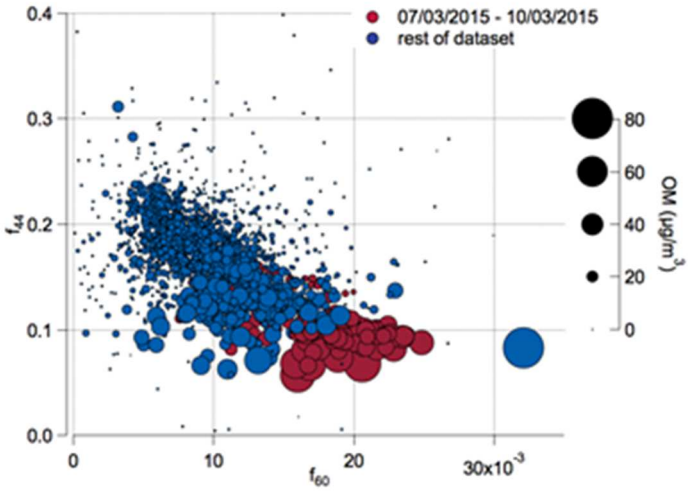

Figure 7: f_{44} vs f_{60} plot in Metz. Marker size is function of OM concentrations

Low temperatures and wind speeds (average of 5.2°C and 0.67 m/s, respectively), combined with the orography of the Moselle valley were favourable to the local/regional pollution built-up during this period. This 4-day episode clearly contributed to the PM "anomaly" for March 2015, as described in Section 3.1. Also, the difference between predicted NH_4 (from ion balance) and measured NH_4 shows in Metz a clearly positive bias during this period (Figures 8a and 8b). There might be several reasons for such as phenomena, including the presence of sulphate in the forms of H_2SO_4 or NH_4HSO_4 (Zhang et al., 2007). However, North of France is considered as displaying excess NH_3, especially in this period of the year (e.g., Fortems-Cheiney et al., 2016; Petetin et al., 2016), so that we can assume H_2SO_4 and NH_4HSO_4 (as well as HNO_3) to be quite limited in the particulate phase. Another possibility might be the significant presence of organonitrate (ON) causing "virtual" nitrate concentrations within ACSM measurements (Farmer et al., 2010). Assuming that the positive bias between predicted and measured ammonium is entirely due to ON only, its concentration can be re-calculated (Farmer et al., 2010). During the wood-burning-dominated sub-episode, ON would then have reached significant concentrations, oscillating around 5 µg/m^3, representing on average 29% of total nitrate (Figure 8c). As highlighted by Kiendler-Scharr et al. (2016) in Europe, this result emphasizes the role of NO_3-based oxidation processes in the formation of secondary organic aerosols. Moreover, enhanced concentrations are observed during the evening and the night, and to a lesser extent during the early morning, suggesting quick formation of radical NO_3.

Then, temporal variabilities observed in Creil and SIRTA differs from what is observed in Lyon or Metz, with a pronounced diurnal profile. The 2 sites have also strong co-variability, in terms of chemical composition and meteorological conditions (T, RH and air mass). Indeed, the sum of the Pearson coefficient r^2 with these parameters ($\sum_i r_i^2$ where i={OM,

NO_3, SO_4, T, RH, cluster}) between the 2 sites is equal to 4.3, with individual r^2 being always above 0.6. This contrasts with the value of 2.25, 2.15, and 2.29 obtained when comparing SIRTA and Metz, SIRTA and Lyon, and Metz and Lyon, respectively. Thus, the pollution episode experienced within the Parisian Basin is rather homogeneous, and in these conditions, measurements performed at SIRTA are representative of a large geographical zone. The "sawtooth" pattern, characterized as intense daily cycles of PM dominated by secondary inorganic aerosols, is somewhat similar to what is usually observed during pollution episodes in China (Jia et al., 2008; Li et al., 2016), and is explained by synoptic cycles, especially the passage of cold fronts. Increasing background, feature associated with these pollution episodes, is however not seen in our case; but, interestingly, the daily PM_1 amplitude is progressively increasing, with a 24-h maximum amplitude going up to 103 and 92 µg/m^3 at SIRTA and Creil, respectively. Also, a dense cloud layer has been observed over Northern France between 19/03 and 21/03 (Figures S3), limiting the amount of sunshine, and thus the convective potential of lower atmospheric layers.

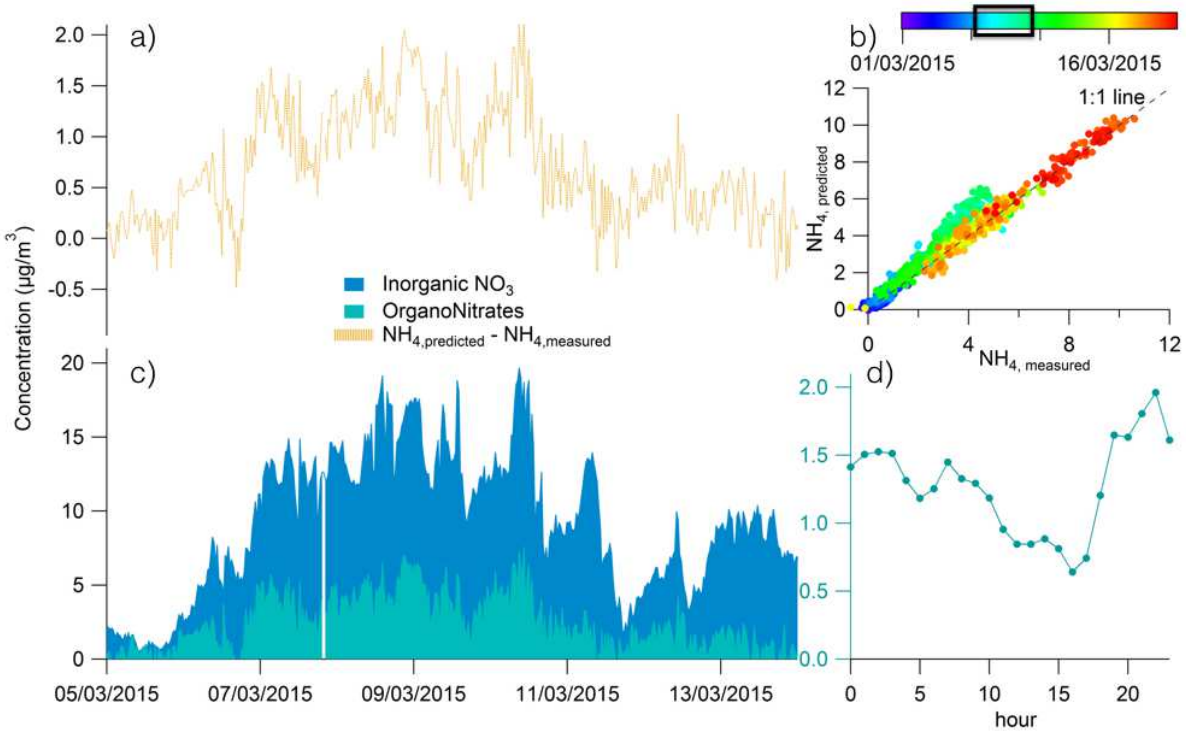

Figure 8. a) Temporal variations of the difference between predicted NH_4 from ionic balance and measured NH_4; b) predicted NH_4 versus measured NH_4. Markers are color-coded by the date, the black box refers to the period from 06/3 to 10/03; c) calculated organonitrates and inorganic nitrate; d) average diurnal variation of calculated organonitrates.

Aerosol aging can be highlighted during this pollution episode when comparing organic f_{44} versus f_{43} (Ng et al., 2011b) averages change from a period to another (Figure 9). Within Oxidized Organic Aerosols (OOA), m/z 44 is mostly relative to acids and acid-derived compounds (Duplissy et al., 2011), while m/z 43 mainly refers to $C_2H_3O^+$ and originates from non-acid oxidation products. Crenn et al. (2015) and Fröhlich et al. (2015) have shown a large variability in f_{44} signals between ACSMs making the intercomparability prone to non-negligible uncertainties; however, it doesn't prevent from interpreting the change of this ratio from a single instrument. Also, Pieber et al. (2016) have recently pointed out f_{44} contributions from ammonium nitrate which could cause an overestimation of the m/z signal, and

accordingly proposed a correction in the fragmentation table based on calibration data. Tests on ACSMs of SIRTA and Metz showed very little influence of this artefact: indeed, comparison of f_{44} with and without correction gave slopes respectively equal to 1.0014 and 0.9998, with r^2 higher than 0.99. Two distinct periods, March 13-14-15 and March 18-19-20, were used to calculated average organic fractions (Figure 9). All sites have average f_{44} at least higher than 0.15, meaning that f_{44} is during these periods more relative of OOA rather than Hydrocarbon-like Organic Aerosol (HOA) (Ng et al., 2011b). SIRTA and Creil exhibit a substantial change in particulate organic composition, since f_{44} has increased values during the most intense part of the pollution episode, concomitantly with a decrease of f_{43}. This is characteristic of an increase of O:C ratio and also the contribution of Low-Volatility Oxidized Organic Aerosol (LV-OOA). This change supports the finding of Morgan et al. (2010), where flights over Europe have highlighted significant transformation occurred, especially regarding secondary organic aerosols. The geographical coverage of this study does not offer the possibility to determine where these oxidation processes occurred, but the observed significant change in f_{43} vs f_{44} space occurred when the origin of air masses also changes from NE to N. Given the relatively high wind speeds (average of 11.1 km/h between 18/03 and 21/03 at SIRTA), this indicates advection of aged aerosols over the Parisian basin. Interestingly, no change is noticeable in Lyon and Metz, suggesting that submicron organic aerosol composition have remained relatively constant, or, at least, with the same oxidation properties. Metz and Lyon have therefore been less impacted by long-range advection.

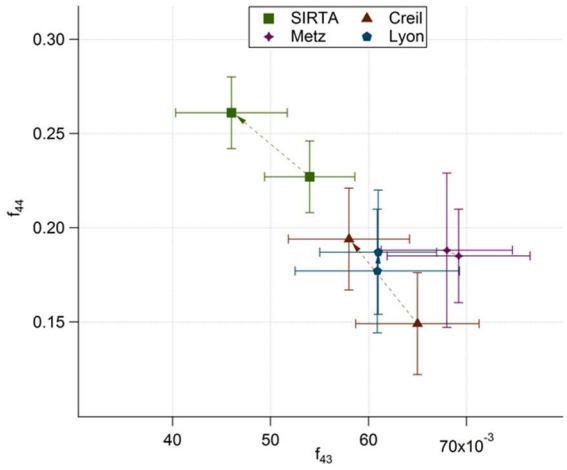

Figure 9: Change of f_{44} relatively to f_{43} at all sites between March 13-14-15 and March 18-19-20. Error bars are ± 1σ.

The PM_1 fraction dominates PM_{10} at all sites, representing around 66%, 61% and 56% on average respectively in SIRTA, Metz and Lyon, but the other interesting feature also lies in the increase of the fraction between 1 and 2.5 µm during the episode. PM_1 is the sum of all chemical components measured by both ACSM and AE33; $PM_{2.5}$ and PM_{10} were retrieved from TEOM-FDMS measurements (Figure 10). $PM_{1\text{-}2.5}$ and $PM_{2.5\text{-}10}$ are thus calculated by direct subtraction. At SIRTA, this increase started on March 16th and stayed rather constant throughout the episode, while it appeared in Metz on March 19th. It is another indicator of significant aging of aerosols. The rather flat pattern of $PM_{1\text{-}2.5}$ over the day in Lyon and SIRTA should be related to rather low volatile compounds. Suggested from Figure 8, organic matter in this fraction could be more oxidized, although no direct measurements can support this hypothesis. Lyon experienced poor variations in f_{44} comparatively to f_{43}, concomitantly with $PM_{1\text{-}2.5}$ fraction being fairly constant in terms of contribution.

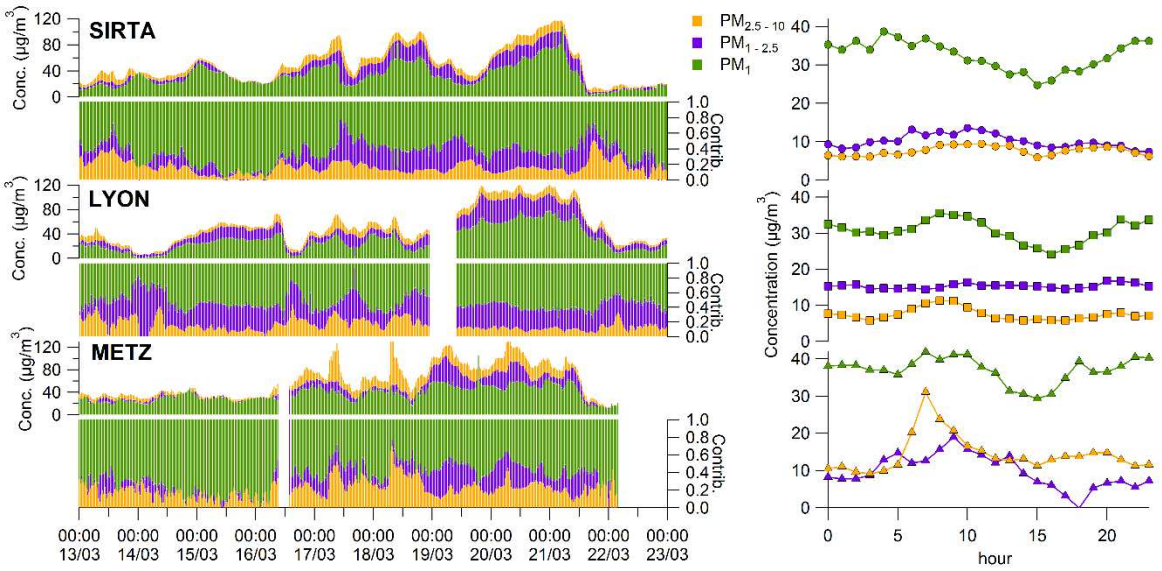

Figure 10: Temporal variations of PM_1, $PM_{1\text{-}2.5}$ and $PM_{2.5\text{-}10}$ fractions in SIRTA, Lyon and Metz between 13/03/2015 and 23/03/2015.

3.4. Geographical origins

From above results, concentrations measured at SIRTA during this large scale episode can be representative of a large geographical window in the Parisian basin. However, since no BC data are available in Creil, Creil data will not be considered hereinafter.

Figure 11 presents the results of the CWT analysis on NO_3 and SO_4 in SIRTA, Lyon and Metz. 3-h concentration data were used, which result in a 240-point dataset for each site. The temporal variabilities described in Section 3.2. ensure the statistical representativeness of the results. Two maps are merged together for each pollutant at each site: "Total" refers to the entire dataset, while "local/regional" corresponds to a subset associated to low wind speed.

For sulphate, CWT strengthens the rather advected pattern commonly observed in Western Europe. Indeed, Pay et al., (2012) have shown that Belgium, Netherlands and Western Germany are an intense and wide-spread zone of SO_2 emissions. Bressi et al. (2014) and Waked et al. (2014) have also shown that SO_4 concentrations, respectively measured in Paris (France) and Lens (France), are largely influenced by these regions. Here, the striking feature lies in the fact that no similarities in terms of geographical origin are found at SIRTA, Metz and Lyon, meaning that they are impacted by different air parcels, and thus potentially by different kind of sources. This is of prime interest because it reinforces the idea of site-to-site discrepancies, and shall be linked to the topoclimatology. Indeed, for SIRTA, a clear hotspot is localized around the mouth of the Rhine River, where intense shipping and industrial activities (notably petrochemical refining) occur. Whereas for Metz, emissions, which could originate from Eastern Germany/Northern Czech Republic, and probably Western Poland, potentially from coal-fired power stations, may be highlighted. These regions are identified as strong SO_2 emitters, from the 2005 European emission inventory (http://www.eea.europa.eu/data-and-maps/figures/so2-annual-average-2005) and Pay et al. (2012). Finally, for Lyon, estimated concentrations follow a quasi-straight pattern through the Rhone, Moselle and Ruhr valley, the latter one hosting heavy industrial activities. Contributions of local/regional concentrations are relatively low, especially at SIRTA, which is consistent with the advected pattern of SO_4. Higher contributions are observed in Metz and Lyon (up to around 1 µg/m^3), probably due to a higher persistence of air masses in these

regions, which allows the formation of ammonium sulphate on a regional scale.

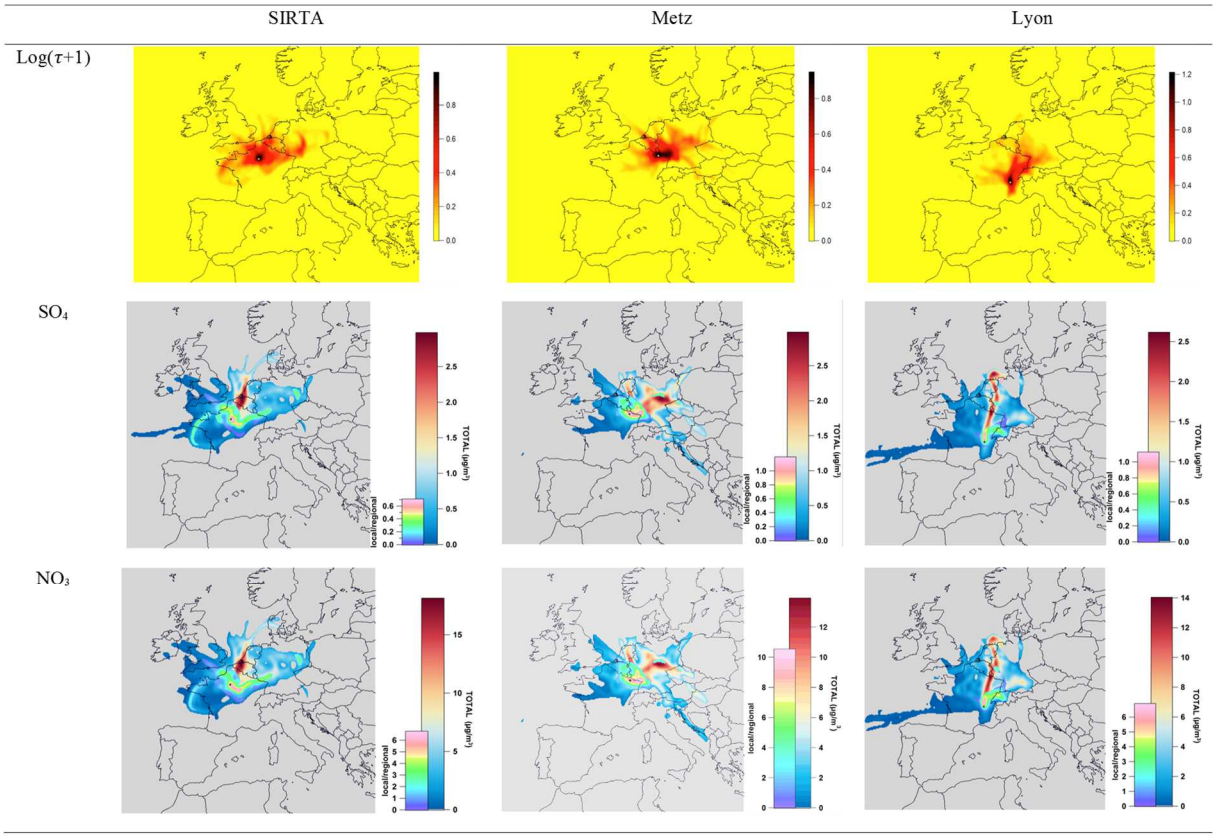

Figure 11: CWT maps for SO_4 and NO_3, at SIRTA, Metz and Lyon. "Total" is the entire dataset; "local/regional" is the subset associated with low wind speed values. Scale sizes for "local/regional" are proportional. Log(τ+1) represent the trajectory density (occurrence of backtrajectory endpoints which fall into a particular cell (colorbar has no unit)

Similar maps are obtained for nitrate, which highlight one of the limits of trajectory analyses applied to secondary pollutants, especially on particulate nitrate and sulphate, because these two compounds have a different formation chemistry, and the sources of their precursors may differ. This result is observed mainly because nitrate and sulphate concentrations are relatively well correlated in time: r^2 of 0.76, 0.59 and 0.89 are respectively observed at SIRTA, Metz and Lyon when comparing nitrate and sulphate timeseries. High concentrations of both compounds are thus attributed to the same backtrajectories. Pay et al. (2012) still report high NO_x emissions in Northern Belgium and Netherlands, so even if the sources are different, a conjoint emission zone is conceivable. The most interesting feature for nitrate lies in the fact that contributions at low wind speeds are much higher, going up to around 7, 10 and 7 µg/m^3 in SIRTA, Metz and Lyon, respectively, being around 40%, 80% and 45% of the total. This emphasizes a significant role on average of local/regional formation of ammonium nitrate, especially in the region of Metz.

Forcing backtrajectories with local/regional concentrations represents a unique opportunity to evaluate their impacts on the total result. For example, at SIRTA, highest concentrations of "local signal" are displayed on the South-East of the receptor site, and is the consequence of the path of the associated trajectories. Previous PSCF results for Paris, published in Bressi et al. (2014) have shown potential areas for road traffic and biomass burning located on the

South of Paris; in Lens, Waked et al. (2014) have shown biomass burning on the SE, although these sources are believed to be quite local. Thus, these observations could just be the outcome of enhanced measured concentrations during stagnant air masses, and should not necessarily be representative of the highlighted air parcels. This finally emphasizes the need of removing these periods from any trajectory-based approach, which can be done with a wind speed threshold, or by prior identification of trajectory clusters; and would also need to be cross-validated by emission scenarios through CTMs.

3.5. Model evaluation

Figure 12 presents the Normal Mean Bias and correlation r values for each major chemical component at each site. Although presented here for the sake of consistency, discrepancies observed for OM will not be discussed, as simulated concentrations were obtained with a CHIMERE simulation issued from the PREV'AIR forecasting system (Rouil et al., 2009), excluding the Volatility-Basis Set, introduced by Zhang et al. (2013). The volatility of Primary Organic Aerosol as well as aging of semi-volatile organic compounds are thus not taken into account, mainly because the emissions of these species are very uncertain. In Europe, the main lack is probably attributed to wood burning emissions; Denier van der Gon et al. (2015) proposed an updated version of the European inventory doubling at least the organic matter emissions from residential emissions compared to standard official emissions if SVOC emissions are included. Previous model evaluation exercises on organics have already highlighted strong underestimation, linked to the amount of Secondary Organic Aerosols (Bessagnet et al., 2016). To perform such a work, prior organic source apportionment is critical, and should thus be presented in another dedicated study.

Black carbon is strongly overestimated at SIRTA by more than 60%, correlating with previous evaluations at SIRTA that have already been reported by Petetin et al. (2014) and Petetin et al. (2015) for the entire Paris region and by Sciare et al. (2011) in downtown Paris during a springtime pollution episode, and Zhang et al. (2013) during the MEGAPOLI campaign. At the same time, BC is inversely strongly underestimated at Metz and Lyon (-79.1% and -68.5% respectively). Diurnal variations (Figure S9) shows however satisfying correlation with a bimodal pattern, linked to daily commuting (i.e. traffic) with the evening peak being enhanced by wood-burning emissions; R values for the entire dataset are between 0.5 and 0.74. Therefore, if a homogenous error is made on emission factors at the national scale, the discrepancies observed here shall be related to a misknowledge of source activities (mainly traffic and wood-burning).

NMB values for nitrate range from -4.8% to -18%, which is satisfactory given the complexity of nitrate formation, and that ammonium nitrate is the major compound of submicron aerosol during most pollution episodes in these periods. From diurnal variations, night-times formation is also well simulated at all sites, meaning that the chemical processes governing the formation of ammonium nitrate are well described by the model. In Paris, the regional contribution of nitrate has been previously found to be overestimated over Paris region on an annual basis (Petetin et al., 2014). Here, the highest concentrations appear to be underestimated by about 10 to 30 $\mu g/m^3$ in absolute values (Figure S7), although temporal homogeneity in the chemical composition over the Parisian Basin, trajectory analysis and f_{44} vs f_{43} space underline a significant advected pattern in this region. Nitrate underestimation have been shown during a springtime pollution episode with continental influence in 2007 in the Paris area (Sciare et al., 2010) and also in Bessagnet et al. (2005). This is similar to significant discrepancies observed in pollution episodes between 2011 and 2013 in terms of meteorology, chemical composition and variability (Petit et al., 2015), and that model performance for nitrate may be episode-dependent. Another dependence may be the origin of

air masses, because they are associated with specific meteorological conditions, chemical transformations and long-distance sources.

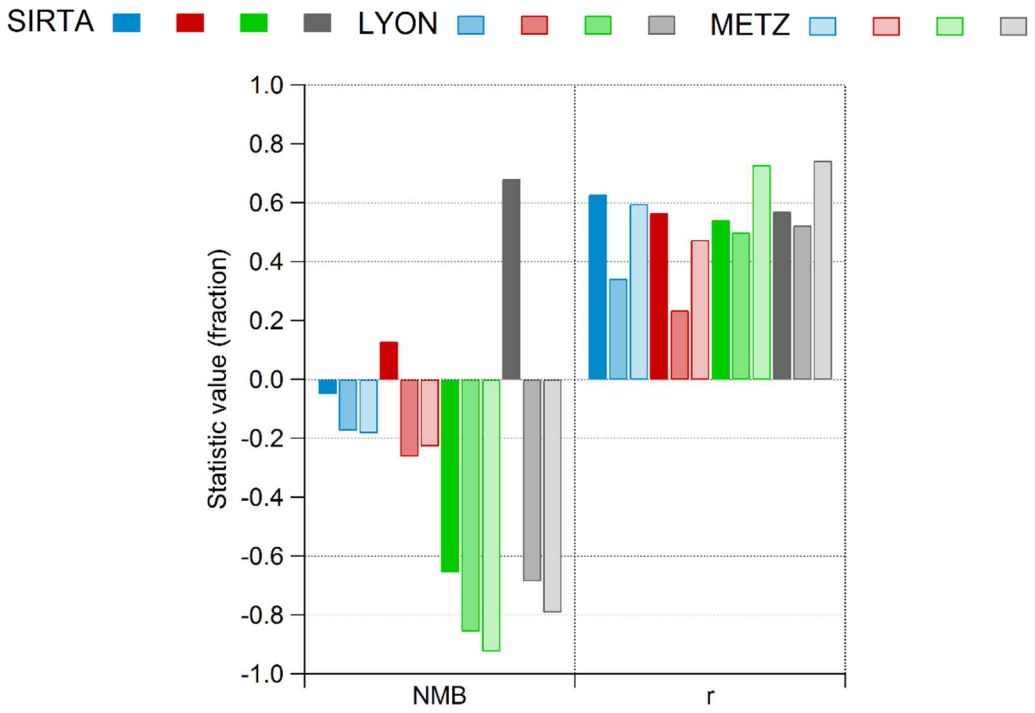

Figure 12: Normalized Mean Bias (NMB) and Pearson coefficients (r) between observed and modelled concentrations of NO_3 (blue), SO_4 (red), OM (green) and BC (black) at SIRTA, Lyon and Metz.

Figure 13 illustrates the influence of the air mass origin on the performance of the model (NMB statistic for NO_3 and SO_4 datasets, divided by the different clusters). Large NMB values are shown for oceanic air masses, but are usually associated with low concentrations in average, making the absolute bias low. The missing coarse nitrate processes in the model could explain the overestimation of ammonium nitrate formation under westerly wind conditions, sodium should compete with ammonium to produce coarser particles that have shorter life time. Following other more polluted air masses (from N to E), model performance changes, without any pattern from a sampling site to another one: Northern cluster is associated to an underestimation of NO_3 at SIRTA and in Metz (-50% and -40%, respectively), while it is overestimated in Lyon (+42%). In Metz, nitrate was relatively well simulated during the episode at the beginning of the month, which were characterized by stagnant air masses, low temperatures, and a predominance of local sources (Figure S7). However, the performances are significantly impaired from March 19th to 21st, where the advection and aging processes occurred. These results are in line with Bessagnet et al. (2014) who reported a general underestimation of nitrate concentrations for the highest values, and an overestimation of the lowest concentrations, leading to global good performance on average.

Similarly to nitrate, modelled sulphate agrees relatively well with observations, NMB ranging from -26.1% in Lyon to +13% at SIRTA. CHIMERE also failed at reconstructing SO_4 concentrations in Lyon during the most intense part of the pollution episode; explaining the poor time correlation coefficient of 0.22 at this site for this pollutant. Diurnal variations also

display a systematic trend for modelled SO_4 (Figure S8), with a substantial increase during the morning, and continuous slight decrease during the afternoon, contrasting with the rather flat pattern of the observed concentrations. This may be linked to SO_2 diurnal emissions used in CHIMERE (not shown here) that also exhibit such an increase.

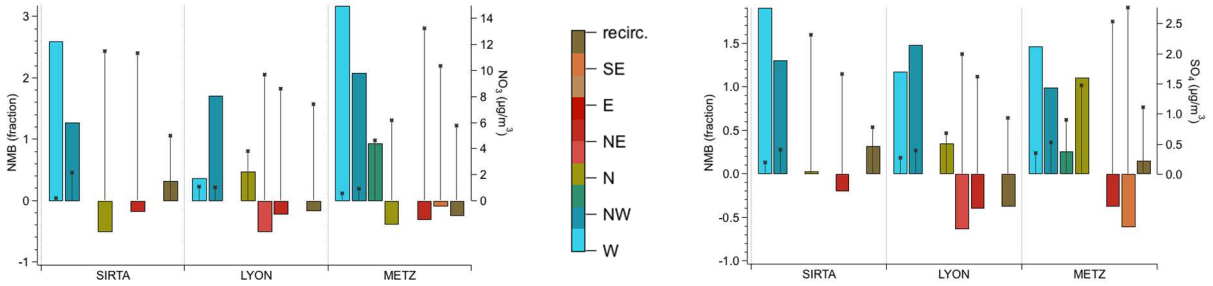

Figure 13: NMB values (bars) and average concentration (stick and markers) of NO_3 and SO_4 following the different air mass origins of Figure 2.

4. Conclusion

The present study investigates, for the first time in France, the spatiotemporal variability of an intense PM pollution episode, which occurred during March 2015. State-of-the-art instrumentation provided near real-time information of the chemical composition of submicron aerosols at four different sampling sites across the country (Paris, Creil, Lyon and Metz).

The first noticeable feature of this episode is the low amount of rainfall compared to normal at all sites. Rain shortage have been also associated with most of unusual PM_{10} monthly concentrations during spring since 2007. Previous climatological studies have shown that precipitation frequency, more than temperature, controls the evolution of PM concentrations over time; we showed here the influence of springtime droughts, which are linked to PM exceedances through pollution episodes. Moreover, climatic predictions appear to be unfavourable, and could facilitate a bit more the formation of pollution episodes in France during spring; meaning that additional efforts on emission controls would need to be made in order to thwart this risk factor. This is one of the few climatology analysis applied to PM pollution episode in France, or even in Europe, therefore this kind of study would need to be extended to a wider spatiotemporal scale.

This PM pollution episode can be considered as large-scale because the increase of PM concentration was observed nationwide at around the same moment. More specifically, ammonium nitrate dominated the PM_1 chemical composition during most of the episode, which is a feature that is now commonly observed in Western Europe during spring. From trajectory analyses, we have shown that transboundary advection had a clear influence on NH_4NO_3 measured in Paris and Creil, still emphasizing international efforts of cooperation to better constrain our understanding of pollution formation. Also, aerosol aging was highlighted through the increase, in SIRTA, Lyon and Metz, of the contribution of the $PM_{1\text{-}2.5}$ fraction. In Metz and SIRTA, the periods when $PM_{1\text{-}2.5}$ respectively increased also correspond to the periods when loss of automatic compensation with AE33 measurements were observed. There shall be no causal link between these two facts at this stage, but should be further investigated, especially regarding the chemical composition of this PM fraction.

If homogeneity is found at SIRTA and Creil regarding chemical composition and temporal variations (sawtooth pattern with strong daily variations), it significantly differs from what was observed elsewhere. In particular, a strong sub-episode occurred in Metz during early

March, when chemical composition was dominated by organic matter and black carbon. f_{60} vs f_{44} distribution, and high BC_{ff} concentrations, respectively emphasize the role of primary local sources, such as wood burning and traffic, during large scale pollution episodes.

Finally, performance of CHIMERE has been evaluated on the selected species (nitrate, sulphate, organic matter and black carbon). Results on secondary inorganics are very satisfactory on average, but hide significant discrepancies from site to site, and also exhibit a dependence on the air mass origin. For instance, nitrate at SIRTA is on average very well modelled, with a normalized mean bias of -4.8%, but weaker performance is observed i) during periods associated with transboundary transport, and ii) in Lyon, where the episode stayed completely unseen. For carbonaceous species, while model performance with organic matter should be performed after source apportionment, BC still reflects a lack of knowledge of the activity and emission factors of certain source, and that this information need to be geographically refined, because site-to-site variability is also observed. The impact of emission inventories, especially regarding secondary pollutants like ammonium nitrate and sulphate, should be further investigated on a larger temporal scale (e.g. a year), with European, national and/or regional inventories.

On a broader perspective, this study suggests the need of spatially resolved real-time data of PM chemical composition. Through the rapid deployment of ACSM and AE33 instruments in France, but also in Europe, and international collaborative efforts, atmospheric phenomenon like transboundary pollution advection should be better documented and constrained over a continental scale. Through large scale evaluations or real-time data assimilation, these in-situ measurements are also great opportunities for building strong connections with modelling studies, which are essential for air quality forecasting but also in our understanding of specific formation processes.

References

Alfarra, M. R., Prevot, A. S. H., Szidat, S., Sandradewi, J., Weimer, S., Lanz, V. A., Schreiber, D., Mohr, M. and Baltensperger, U.: Identification of the mass spectral signature of organic aerosols from wood burning emissions, Environ. Sci. Technol., 41(16), 5770–5777, 2007.

Allan, J. D., Delia, A. E., Coe, H., Bower, K. N., Alfarra, M. R., Jimenez, J. L., Middlebrook, A. M., Drewnick, F., Onasch, T. B., Canagaratna, M. R., Jayne, J. T. and Worsnop, D. R.: A generalised method for the extraction of chemically resolved mass spectra from Aerodyne aerosol mass spectrometer data, J. Aerosol Sci., 35(7), 909–922, doi:10.1016/j.jaerosci.2004.02.007, 2004.

Ashbaugh, L. L., Malm, W. C. and Sadeh, W. Z.: A residence time probability analysis of sulfur concentrations at Grand Canyon National Park, Atmospheric Environ. 1967, 19(8), 1263–1270, 1985.

Beekmann, M., Prévôt, A. S. H., Drewnick, F., Sciare, J., Pandis, S. N., Denier van der Gon, H. A. C., Crippa, M., Freutel, F., Poulain, L., Ghersi, V., Rodriguez, E., Beirle, S., Zotter, P., von der Weiden-Reinmüller, S.-L., Bressi, M., Fountoukis, C., Petetin, H., Szidat, S., Schneider, J., Rosso, A., El Haddad, I., Megaritis, A., Zhang, Q. J., Michoud, V., Slowik, J. G., Moukhtar, S., Kolmonen, P., Stohl, A., Eckhardt, S., Borbon, A., Gros, V., Marchand, N., Jaffrezo, J. L., Schwarzenboeck, A., Colomb, A., Wiedensohler, A., Borrmann, S., Lawrence, M., Baklanov, A. and Baltensperger, U.: In-situ, satellite measurement and model evidence for a~dominant regional contribution to fine particulate matter levels in the Paris Megacity, Atmospheric Chem. Phys. Discuss., 15(6), 8647–8686, doi:10.5194/acpd-15-8647-2015, 2015.

Bessagnet, B., Hodzic, A., Blanchard, O., Lattuati, M., Lebihan, O., Marfaing, H. and Rouil, L.: Origin of particulate matter pollution episodes in wintertime over the Paris Basin, Atmos. Environ., 39(33), 6159–6174, doi:10.1016/j.atmosenv.2005.06.053, 2005.

Bessagnet, B., Pirovano, G., Mircea, M., Cuvelier, C., Aulinger, A., Calori, G., Ciarelli, G., Manders, A., Stern, R., Tsyro, S., García Vivanco, M., Thunis, P., Pay, M.-T., Colette, A., Couvidat, F., Meleux, F., Rouïl, L., Ung, A., Aksoyoglu, S., Baldasano, J. M., Bieser, J., Briganti, G., Cappelletti, A., D'Isidoro, M., Finardi, S., Kranenburg, R., Silibello, C., Carnevale, C., Aas, W., Dupont, J.-C., Fagerli, H., Gonzalez, L., Menut, L., Prévôt, A. S. H., Roberts, P. and White, L.: Presentation of the EURODELTA III intercomparison exercise – evaluation of the chemistry transport models' performance on criteria pollutants and joint analysis with meteorology, Atmospheric Chem. Phys., 16(19), 12667–12701, doi:10.5194/acp-16-12667-2016, 2016.

Briggs, N. L. and Long, C. M.: Critical review of black carbon and elemental carbon source apportionment in Europe and the United States, Atmos. Environ., doi:10.1016/j.atmosenv.2016.09.002, 2016.

Chakraborty, A., Bhattu, D., Gupta, T., Tripathi, S. N. and Canagaratna, M. R.: Real-time measurements of ambient aerosols in a polluted Indian city: Sources, characteristics, and processing of organic aerosols during foggy and nonfoggy periods: REAL-TIME SUBMICRON AEROSOL PROPERTIES, J. Geophys. Res. Atmospheres, 120(17), 9006–9019, doi:10.1002/2015JD023419, 2015.

Crenn, V., Sciare, J., Croteau, P. L., Verlhac, S., Fröhlich, R., Belis, C. A., Aas, W., Äijälä, M., Alastuey, A., Artiñano, B., Baisnée, D., Bonnaire, N., Bressi, M., Canagaratna, M., Canonaco, F., Carbone, C., Cavalli, F., Coz, E., Cubison, M. J., Esser-Gietl, J. K., Green, D. C., Gros, V.,

Heikkinen, L., Herrmann, H., Lunder, C., Minguillón, M. C., Močnik, G., O'Dowd, C. D., Ovadnevaite, J., Petit, J.-E., Petralia, E., Poulain, L., Priestman, M., Riffault, V., Ripoll, A., Sarda-Estève, R., Slowik, J. G., Setyan, A., Wiedensohler, A., Baltensperger, U., Prévôt, A. S. H., Jayne, J. T. and Favez, O.: ACTRIS ACSM intercomparison – Part 1: Reproducibility of concentration and fragment results from 13 individual Quadrupole Aerosol Chemical Speciation Monitors (Q-ACSM) and consistency with co-located instruments, Atmospheric Meas. Tech., 8(12), 5063–5087, doi:10.5194/amt-8-5063-2015, 2015.

Cubison, M. J., Ortega, A. M., Hayes, P. L., Farmer, D. K., Day, D., Lechner, M. J., Brune, W. H., Apel, E., Diskin, G. S., Fisher, J. A., Fuelberg, H. E., Hecobian, A., Knapp, D. J., Mikoviny, T., Riemer, D., Sachse, G. W., Sessions, W., Weber, R. J., Weinheimer, A. J., Wisthaler, A. and Jimenez, J. L.: Effects of aging on organic aerosol from open biomass burning smoke in aircraft and laboratory studies, Atmospheric Chem. Phys., 11(23), 12049–12064, doi:10.5194/acp-11-12049-2011, 2011.

Denier van der Gon, H. A. C., Bergström, R., Fountoukis, C., Johansson, C., Pandis, S. N., Simpson, D. and Visschedijk, A. J. H.: Particulate emissions from residential wood combustion in Europe – revised estimates and an evaluation, Atmospheric Chem. Phys., 15(11), 6503–6519, doi:10.5194/acp-15-6503-2015, 2015.

Draxler, R.: Hysplit4 User's Guide, 1999.

Drinovec, L., Močnik, G., Zotter, P., Prévôt, A. S. H., Ruckstuhl, C., Coz, E., Rupakheti, M., Sciare, J., Müller, T., Wiedensohler, A. and Hansen, A. D. A.: The "dual-spot" Aethalometer: an improved measurement of aerosol black carbon with real-time loading compensation, Atmospheric Meas. Tech., 8(5), 1965–1979, doi:10.5194/amt-8-1965-2015, 2015.

Duplissy, J., DeCarlo, P. F., Dommen, J., Alfarra, M. R., Metzger, A., Barmpadimos, I., Prevot, A. S. H., Weingartner, E., Tritscher, T., Gysel, M., Aiken, A. C., Jimenez, J. L., Canagaratna, M. R., Worsnop, D. R., Collins, D. R., Tomlinson, J. and Baltensperger, U.: Relating hygroscopicity and composition of organic aerosol particulate matter, Atmospheric Chem. Phys., 11(3), 1155–1165, doi:10.5194/acp-11-1155-2011, 2011.

Farmer, D. K., Matsunaga, A., Docherty, K. S., Surratt, J. D., Seinfeld, J. H., Ziemann, P. J. and Jimenez, J. L.: Response of an aerosol mass spectrometer to organonitrates and organosulfates and implications for atmospheric chemistry, Proc. Natl. Acad. Sci., 107(15), 6670–6675, doi:10.1073/pnas.0912340107, 2010.

Favez, O., El Haddad, I., Piot, C., Boréave, A., Abidi, E., Marchand, N., Jaffrezo, J. L., Besombes, J. L., Personnaz, M. B., Sciare, J., Wortham, H., George, C. and D'anna, B.: Inter-comparison of source apportionment models for the estimation of wood burning aerosols during wintertime in an Alpine city (Grenoble, France), Atmos Chem Phys, 10, 5295–5314, doi:10.5194/acp-10-5295-2010, 2010.

Favez, O., Petit, J.-E., Bessagnet, B., Meleux, F., Chiappini, L., Lemeur, S., Labartette, C., Chappaz, C., Guergnion, P.-Y., Saison, J.-Y., Chretien, E., Pallares, C., Verlhac, S., Aujay, R., Malherbe, L., Beauchamp, M., Piot, C., Jaffrezo, J.-L., Besombes, J.-L., Sciare, J., Rouïl, L. and Leoz-Garziandia, E.: Main properties and origines of winter PM10 pollution events in France, Pollut. Atmospherique, 163–182, 2012.

Fortems-Cheiney, A., Dufour, G., Hamaoui-Laguel, L., Foret, G., Siour, G., Van Damme, M., Meleux, F., Coheur, P.-F., Clerbaux, C., Clarisse, L., Favez, O., Wallasch, M. and Beekmann, M.: Unaccounted variability in NH3 agricultural sources detected by IASI contributing to European spring haze episode: Agricultural NH3 Detected by IASI, Geophys. Res. Lett., 43(10), 5475–5482, doi:10.1002/2016GL069361, 2016.

Freney, E. J., Sellegri, K., Canonaco, F., Colomb, A., Borbon, A., Michoud, V., Doussin, J.-F., Crumeyrolle, S., Amarouche, N., Pichon, J.-M., Bourianne, T., Gomes, L., Prevot, A. S. H., Beekmann, M. and Schwarzenböeck, A.: Characterizing the impact of urban emissions on regional aerosol particles: airborne measurements during the MEGAPOLI experiment, Atmospheric Chem. Phys., 14(3), 1397–1412, doi:10.5194/acp-14-1397-2014, 2014.

Fröhlich, R., Crenn, V., Setyan, A., Belis, C. A., Canonaco, F., Favez, O., Riffault, V., Slowik, J. G., Aas, W., Aijälä, M., Alastuey, A., Artiñano, B., Bonnaire, N., Bozzetti, C., Bressi, M., Carbone, C., Coz, E., Croteau, P. L., Cubison, M. J., Esser-Gietl, J. K., Green, D. C., Gros, V., Heikkinen, L., Herrmann, H., Jayne, J. T., Lunder, C. R., Minguillón, M. C., Močnik, G., O'Dowd, C. D., Ovadnevaite, J., Petralia, E., Poulain, L., Priestman, M., Ripoll, A., Sarda-Estève, R., Wiedensohler, A., Baltensperger, U., Sciare, J. and Prévôt, A. S. H.: ACTRIS ACSM intercomparison – Part 2: Intercomparison of ME-2 organic source apportionment results from 15 individual, co-located aerosol mass spectrometers, Atmospheric Meas. Tech., 8(6), 2555–2576, doi:10.5194/amt-8-2555-2015, 2015.

Haeffelin, M., Barthès, L., Bock, O., Boitel, C., Bony, S., Bouniol, D., Chepfer, H., Chiriaco, M., Cuesta, J. and Delanoë, J.: SIRTA, a ground-based atmospheric observatory for cloud and aerosol research, Ann. Geophys., 253–275, 2005.

Herich, H., Hueglin, C. and Buchmann, B.: A 2.5 year's source apportionment study of black carbon from wood burning and fossil fuel combustion at urban and rural sites in Switzerland, Atmospheric Meas. Tech., 4(7), 1409–1420, doi:10.5194/amt-4-1409-2011, 2011.

Huang, R.-J., Zhang, Y., Bozzetti, C., Ho, K.-F., Cao, J.-J., Han, Y., Daellenbach, K. R., Slowik, J. G., Platt, S. M., Canonaco, F., Zotter, P., Wolf, R., Pieber, S. M., Bruns, E. A., Crippa, M., Ciarelli, G., Piazzalunga, A., Schwikowski, M., Abbaszade, G., Schnelle-Kreis, J., Zimmermann, R., An, Z., Szidat, S., Baltensperger, U., Haddad, I. E. and Prévôt, A. S. H.: High secondary aerosol contribution to particulate pollution during haze events in China, Nature, doi:10.1038/nature13774, 2014.

IARC: Outdoor air pollution a leading environmental cause of cancer deaths, press release n°221, 2013.

Jerez, S., Jimenez-Guerrero, P., Montávez, J. P. and Trigo, R. M.: Impact of the North Atlantic Oscillation on European aerosol ground levels through local processes: a seasonal model-based assessment using fixed anthropogenic emissions, Atmospheric Chem. Phys., 13(22), 11195–11207, doi:10.5194/acp-13-11195-2013, 2013.

Jia, Y., Rahn, K. A., He, K., Wen, T. and Wang, Y.: A novel technique for quantifying the regional component of urban aerosol solely from its sawtooth cycles, J. Geophys. Res., 113(D21), doi:10.1029/2008JD010389, 2008.

Jones, P. D. and Lister, D. H.: The influence of the circulation on surface temperature and precipitation patterns over Europe, Clim. Past, 5(2), 259–267, 2009.

Kiendler-Scharr, A., Mensah, A. A., Friese, E., Topping, D., Nemitz, E., Prevot, A. S. H., Äijälä, M., Allan, J., Canonaco, F., Canagaratna, M., Carbone, S., Crippa, M., Dall Osto, M., Day, D. A., De Carlo, P., Di Marco, C. F., Elbern, H., Eriksson, A., Freney, E., Hao, L., Herrmann, H., Hildebrandt, L., Hillamo, R., Jimenez, J. L., Laaksonen, A., McFiggans, G., Mohr, C., O'Dowd, C., Otjes, R., Ovadnevaite, J., Pandis, S. N., Poulain, L., Schlag, P., Sellegri, K., Swietlicki, E., Tiitta, P., Vermeulen, A., Wahner, A., Worsnop, D. and Wu, H.-C.: Ubiquity of organic nitrates from nighttime chemistry in the European submicron aerosol: Organic Nitrates in European PM1, Geophys. Res. Lett., 43(14), 7735–7744, doi:10.1002/2016GL069239, 2016.

Kim, E., Turkiewicz, K., Zulawnick, S. A. and Magliano, K. L.: Sources of fine particles in the South Coast area, California, Atmos. Environ., 44(26), 3095–3100, doi:10.1016/j.atmosenv.2010.05.037, 2010.

Lavers, D., Prudhomme, C. and Hannah, D. M.: European precipitation connections with large-scale mean sea-level pressure (MSLP) fields, Hydrol. Sci. J., 58(2), 310–327, doi:10.1080/02626667.2012.754545, 2013.

Li, H., Duan, F., He, K., Ma, Y., Kimoto, T. and Huang, T.: Size-Dependent Characterization of Atmospheric Particles during Winter in Beijing, Atmosphere, 7(3), 36, doi:10.3390/atmos7030036, 2016.

Menut, L., Bessagnet, B., Khvorostyanov, D., Beekmann, M., Blond, N., Colette, A., Coll, I., Curci, G., Foret, G., Hodzic, A., Mailler, S., Meleux, F., Monge, J.-L., Pison, I., Siour, G., Turquety, S., Valari, M., Vautard, R. and Vivanco, M. G.: CHIMERE 2013: a model for regional atmospheric composition modelling, Geosci. Model Dev., 6(4), 981–1028, doi:10.5194/gmd-6-981-2013, 2013.

Middlebrook, A. M., Bahreini, R., Jimenez, J. L. and Canagaratna, M. R.: Evaluation of Composition-Dependent Collection Efficiencies for the Aerodyne Aerosol Mass Spectrometer using Field Data, Aerosol Sci. Technol., 46(3), 258–271, doi:10.1080/02786826.2011.620041, 2012.

Nenes, A., Pandis, S. N. and Pilinis, C.: ISORROPIA: A new thermodynamic equilibrium model for multiphase multicomponent inorganic aerosols, Aquat. Geochem., 4(1), 123–152, 1998.

Ng, N. L., Herndon, S. C., Trimborn, A., Canagaratna, M. R., Croteau, P. L., Onasch, T. B., Sueper, D., Worsnop, D. R., Zhang, Q. and Sun, Y. L.: An aerosol chemical speciation monitor (ACSM) for routine monitoring of the composition and mass concentrations of ambient aerosol, Aerosol Sci. Technol., 45(7), 780–794, 2011a.

Ng, N. L., Canagaratna, M. R., Jimenez, J. L., Chhabra, P. S., Seinfeld, J. H. and Worsnop, D. R.: Changes in organic aerosol composition with aging inferred from aerosol mass spectra, Atmospheric Chem. Phys., 11(13), 6465–6474, doi:10.5194/acp-11-6465-2011, 2011b.

Ortega, A. M., Day, D. A., Cubison, M. J., Brune, W. H., Bon, D., de Gouw, J. A. and Jimenez, J. L.: Secondary organic aerosol formation and primary organic aerosol oxidation from biomass-burning smoke in a flow reactor during FLAME-3, Atmospheric Chem. Phys., 13(22), 11551–11571, doi:10.5194/acp-13-11551-2013, 2013.

Pausata, F. S. R., Pozzoli, L., Dingenen, R. V., Vignati, E., Cavalli, F. and Dentener, F. J.: Impacts of changes in North Atlantic atmospheric circulation on particulate matter and human health in Europe: NAO IMPACTS ON PM AND HUMAN HEALTH, Geophys. Res. Lett., 40(15), 4074–4080, doi:10.1002/grl.50720, 2013.

Pay, M. T., Jiménez-Guerrero, P. and Baldasano, J. M.: Assessing sensitivity regimes of secondary inorganic aerosol formation in Europe with the CALIOPE-EU modeling system, Atmos. Environ., 51, 146–164, doi:10.1016/j.atmosenv.2012.01.027, 2012.

Petetin, H., Beekmann, M., Sciare, J., Bressi, M., Rosso, A., Sanchez, O. and Ghersi, V.: A novel model evaluation approach focusing on local and advected contributions to urban PM2.5 levels – application to Paris, France, Geosci. Model Dev., 7(4), 1483–1505, doi:10.5194/gmd-7-1483-2014, 2014.

Petetin, H., Beekmann, M., Colomb, A., Denier van der Gon, H. A. C., Dupont, J.-C., Honoré, C., Michoud, V., Morille, Y., Perrussel, O., Schwarzenboeck, A., Sciare, J., Wiedensohler, A. and Zhang, Q. J.: Evaluating BC and NOx emission inventories for the Paris region from MEGAPOLI aircraft measurements, Atmospheric Chem. Phys., 15(17), 9799–9818, doi:10.5194/acp-15-9799-2015, 2015.

Petetin, H., Sciare, J., Bressi, M., Gros, V., Rosso, A., Sanchez, O., Sarda-Estève, R., Petit, J.-E. and Beekmann, M.: Assessing the ammonium nitrate formation regime in the Paris megacity and its representation in the CHIMERE model, Atmospheric Chem. Phys., 16(16), 10419–10440, doi:10.5194/acp-16-10419-2016, 2016.

Petit, J.-E., Favez, O., Sciare, J., Canonaco, F., Croteau, P., Močnik, G., Jayne, J., Worsnop, D. and Leoz-Garziandia, E.: Submicron aerosol source apportionment of wintertime pollution in Paris, France by double positive matrix factorization (PMF^2) using an aerosol chemical speciation monitor (ACSM) and a multi-wavelength Aethalometer, Atmospheric Chem. Phys., 14(24), 13773–13787, doi:10.5194/acp-14-13773-2014, 2014.

Petit, J.-E., Favez, O., Sciare, J., Crenn, V., Sarda-Estève, R., Bonnaire, N., Močnik, G., Dupont, J.-C., Haeffelin, M. and Leoz-Garziandia, E.: Two years of near real-time chemical composition of submicron aerosols in the region of Paris using an Aerosol Chemical Speciation Monitor (ACSM) and a multi-wavelength Aethalometer, Atmospheric Chem. Phys., 15(6), 2985–3005, doi:10.5194/acp-15-2985-2015, 2015.

Pieber, S. M., El Haddad, I., Slowik, J. G., Canagaratna, M. R., Jayne, J. T., Platt, S. M., Bozzetti, C., Daellenbach, K. R., Fröhlich, R., Vlachou, A., Klein, F., Dommen, J., Miljevic, B., Jiménez, J. L., Worsnop, D. R., Baltensperger, U. and Prévôt, A. S. H.: Inorganic Salt Interference on CO2+ in Aerodyne AMS and ACSM Organic Aerosol Composition Studies, Environ. Sci. Technol., doi:10.1021/acs.est.6b01035, 2016.

Pokrovsky, O. M.: European rain rate modulation enhanced by changes in the NAO and atmospheric circulation regimes, Comput. Geosci., 35(5), 897–906, doi:10.1016/j.cageo.2007.12.005, 2009.

Pope, R. J., Savage, N. H., Chipperfield, M. P., Ordóñez, C. and Neal, L. S.: The influence of synoptic weather regimes on UK air quality: regional model studies of tropospheric column NO2;, Atmospheric Chem. Phys., 15(19), 11201–11215, doi:10.5194/acp-15-11201-2015, 2015.

Putaud, J.-P., Van Dingenen, R., Alastuey, A., Bauer, H., Birmili, W., Cyrys, J., Flentje, H., Fuzzi, S., Gehrig, R., Hansson, H.-C. and others: A European aerosol phenomenology–3: Physical and chemical characteristics of particulate matter from 60 rural, urban, and kerbside sites across Europe, Atmos. Environ., 44(10), 1308–1320, 2010.

Ramgolam, K., Favez, O., Cachier, H., Gaudichet, A., Marano, F., Martinon, L. and Baeza-Squiban, A.: Size-partitioning of an urban aerosol to identify particle determinants involved in the proinflammatory response induced in airway epithelial cells, Part. Fibre Toxicol., 6(10), doi:10.1186/1743-8977-6-10, 2009.

Rouil, L., Honoré, C., Bessagnet, B., Malherbe, L., Meleux, F., Vautard, R., Beekmann, M., Flaud, J.-M., Dufour, A., Martin, D., Peuch, A., Peuch, V.-H., Elichegaray, C., Poisson, N. and Menut, L.: Prev'air: An Operational Forecasting and Mapping System for Air Quality in Europe, Bull. Am. Meteorol. Soc., 90(1), 73–83, doi:10.1175/2008BAMS2390.1, 2009.

Rouïl, L., Bessagnet, B., Favez, O., Leoz-Garziandia, E. and Meleux, F.: Particulate air pollution episodes in France: lessons learnt from recent episodes, Pollut. Atmos., 101, 2015.

Sandradewi, J., Prévôt, A. S. H., Szidat, S., Perron, N., Alfarra, M. R., Lanz, V. A., Weingartner, E. and Baltensperger, U.: Using Aerosol Light Absorption Measurements for the Quantitative Determination of Wood Burning and Traffic Emission Contributions to Particulate Matter, Environ. Sci. Technol., 42(9), 3316–3323, doi:10.1021/es702253m, 2008.

Schneider, J., Weimer, S., Drewnick, F., Borrmann, S., Helas, G., Gwaze, P., Schmid, O., Andreae, M. O. and Kirchner, U.: Mass spectrometric analysis and aerodynamic properties of various types of combustion-related aerosol particles, Int. J. Mass Spectrom., 258(1-3), 37–49, doi:10.1016/j.ijms.2006.07.008, 2006.

Sciare, J., d' Argouges, O., Sarda-Estève, R., Gaimoz, C., Dolgorouky, C., Bonnaire, N., Favez, O., Bonsang, B. and Gros, V.: Large contribution of water-insoluble secondary organic aerosols in the region of Paris (France) during wintertime, J. Geophys. Res. Atmospheres, 116(D22), n/a–n/a, doi:10.1029/2011JD015756, 2011.

Stein, A. F., Draxler, R. R., Rolph, G. D., Stunder, B. J. B., Cohen, M. D. and Ngan, F.: NOAA's HYSPLIT Atmospheric Transport and Dispersion Modeling System, Bull. Am. Meteorol. Soc., 96(12), 2059–2077, doi:10.1175/BAMS-D-14-00110.1, 2015.

Waked, A., Favez, O., Alleman, L. Y., Piot, C., Petit, J.-E., Delaunay, T., Verlinden, E., Golly, B., Besombes, J.-L., Jaffrezo, J.-L. and Leoz-Garziandia, E.: Source apportionment of PM10 in a north-western Europe regional urban background site (Lens, France) using positive matrix factorization and including primary biogenic emissions, Atmospheric Chem. Phys., 14(7), 3325–3346, doi:10.5194/acp-14-3325-2014, 2014.

Wang, H.-J. and Chen, H.-P.: Understanding the recent trend of haze pollution in eastern China: roles of climate change, Atmospheric Chem. Phys., 16(6), 4205–4211, doi:10.5194/acp-16-4205-2016, 2016.

Von der Weiden-Reinmüller, S.-L., Drewnick, F., Zhang, Q. J., Freutel, F., Beekmann, M. and Borrmann, S.: Megacity emission plume characteristics in summer and winter investigated by mobile aerosol and trace gas measurements: the Paris metropolitan area, Atmospheric Chem. Phys. Discuss., 14(8), 11249–11299, doi:10.5194/acpd-14-11249-2014, 2014.

Yiou, P. and Cattiaux, J.: Contribution of Atmospheric circulation to wet North European summer precipitation of 2012, Am. Meteorol. Soc., 2013.

Zhang, Q., Jimenez, J. L., Worsnop, D. R. and Canagaratna, M.: A Case Study of Urban Particle Acidity and Its Influence on Secondary Organic Aerosol, Environ. Sci. Technol., 41(9), 3213–3219, doi:10.1021/es061812j, 2007.

Zhang, Q., Yan, R., Fan, J., Yu, S., Yang, W., Li, P., Wang, S., Chen, B., Liu, W. and Zhang, X.: A Heavy Haze Episode in Shanghai in December of 2013: Characteristics, Origins and Implications, Aerosol Air Qual. Res., 15, 1881–1893, doi:10.4209/aaqr.2015.03.0179, 2015.

Zhang, Y., Ding, A., Mao, H., Nie, W., Zhou, D., Liu, L., Huang, X. and Fu, C.: Impact of synoptic weather patterns and inter-decadal climate variability on air quality in the North China Plain during 1980–2013, Atmos. Environ., 124, 119–128, doi:10.1016/j.atmosenv.2015.05.063, 2016.

Zotter, P., Herich, H., Gysel, M., El-Haddad, I., Zhang, Y., Močnik, G., Hüglin, C., Baltensperger, U., Szidat, S. and Prévôt, A. S. H.: Evaluation of the absorption Ångström exponents for traffic and wood burning in the Aethalometer based source apportionment using radiocarbon measurements of ambient aerosol, Atmospheric Chem. Phys. Discuss., 1–29, doi:10.5194/acp-2016-621, 2016.

ANNEXE 2

Description des sites et méthodologies de spéciation chimique utilisés pour l'obtention des jeux de données étudiés dans le cadre de l'analyse PMF harmonisée du projet SOURCES

Site de mesure	Code	Coordonnées	Période de collecte	Nombre d'échantillons	Typologie
Talence	TAL	44°48'2.01"N 0°35'17.01"O	02/02/2012→ 07/04/2013	154	urbain
Lyon	LY	45°45'27.82"N 4°51'15.15"E	03/01/2012→ 31/12/2012	115	urbain
Poitiers	POI	46°34'48.80"N 0°20'25.34"E	16/11/2014→ 29/12/2015	110	urbain
Nice	NIC	43°42'7.48"N 7°17'10.53"E	04/06/2014→ 29/06/2016	184	urbain
Marseille	MRS	43°18'18.84"N 5°23'40.89"E	11/01/2015→ 27/06/2016	102	urbain
Port de Bouc	PdB	43°24'7.99"N 4°58'55.99"E	01/06/2014→ 27/06/16	185	urbain
Aix-en-Provence	PROV	43°31'49.04"N 5°26'29.00"E	18/07/2013→ 13/07/2014	56	urbain
Nogent	NGT	49°16'35.0"N 2°28'56.0"E	02/01/2013→ 02/06/2014	155	urbain
Rouen	ROU	49°25'41.4"N 1°03'29.1"E	02/01/2013→ 01/06/2014	162	urbain
Lens	LEN	50°26'12.6"N 2°49'36.7"E	02/01/2013→ 01/06/2014	167	urbain
Grenoble LF	GRE	45°9'42.84"N 5°44'8.15"E	02/01/2013→ 29/12/2014	240	urbain
Roubaix	RBX	50°42'23.6"N 3°10'50.5"E	20/01/2013→ 26/05/2014	157	trafic
Strasbourg	STRAS	48°34'24.25"N 7°45'7.6"E	02/04/2013→ 08/04/2014	78	trafic
Chamonix	CHAM	45°55'21"N 6°52'12"E	02/11/2013→ 31/10/2014	115	vallée alpine
Revin	REV	49°55'00.0"N 4°38'29.0"E	02/01/2013→ 01/06/2014	168	rural

Le code couleur indique la typologie du site : jaune pour urbain (N=11), rouge pour trafic (N=2), vert clair pour rural (N=1), et marron pour vallée alpine (N=1).

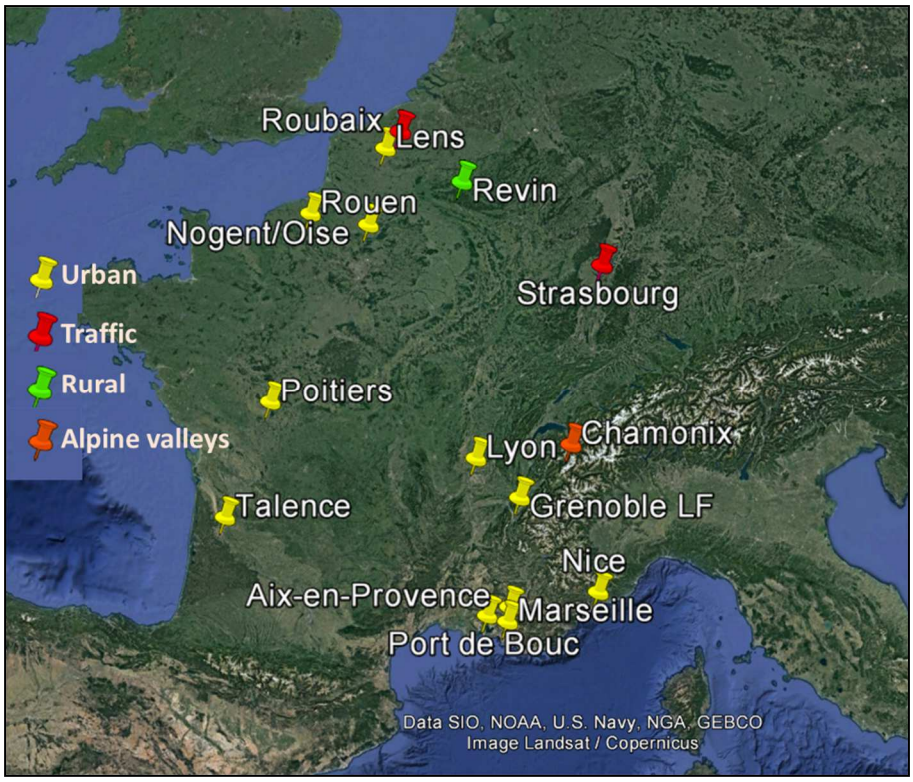

Localisation des 15 sites de mesure exploités dans le cadre du projet « SOURCES ».

Measured species	Analytical method	References
Carbone organique et élémentaire OC, EC	**TOT** (analyse thermo-optique en transmission) à l'aide du Sunset lab analyzer (EUSAAR2 protocol)	(Cavalli et al., 2010)
Espèces solubles majeures SO_4^{2-}, NO_3^-, Cl^-, NH_4^+, Na^+, K^+, Ca^{2+}, Mg^{2+}, MSA, oxalate	**IC** (Chromatographie ionique)	(Jaffrezo et al., 2005)
Métaux et metalloïdes Al, As, Ba, Ca, Cd, Ce, Co, Cr, Cs, Cu, Fe, K, La, Li, Mg, Mn, Mo, Na, Ni, Pb, Pd, Pt, Rb, Sb, Sc, Se, Sn, Sr, Ti, Tl, V, Zn, Zr	**ICP-MS** (inductively coupled plasma mass spectrometry) et **ICP-AES** (inductively coupled atomic emission spectrometry) après digestion acide	(Alleman et al., 2010; Waked et al., 2014)
Sucres - levoglucosan, mannosan, galactosan - arabitol, mannitol, sorbitol	**HPLC-PAD** (high performance liquid chromatography coupled to a pulsed amperometric detection)	(Sciare et al., 2011; Waked et al., 2014)

Méthodologies de spéciation chimique des PM_{10}

Présentation du programme CARA lors de la conférence *Monitoring Ambient Air* 2016 (Londres, 12-13 décembre 2016).

Characterization of PM pollution within the French CARA program

O. Favez, T. Amodeo, A. Albinet, J.E. Petit, B. Bessagnet, A . Colette, J.L. Jaffrezo, J. Savarino, E. Freney, V. Gros

olivier.favez@ineris.fr

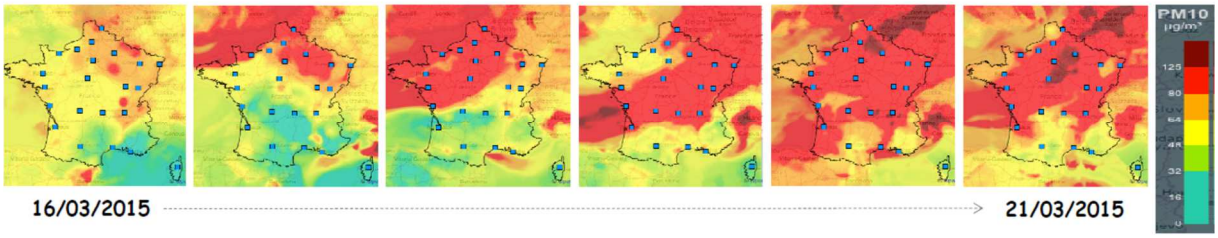

INERIS, Verneuil en Halatte, France
LSCE, Gif sur Yvette, France
LGGE, Saint Martin d'Hères, France
LaMP, Aubières, France

The CARA program

INERIS internal research program

Ph-D « On-line Chemistry » J.E. Petit (2011-2014) INERIS / LSCE

Ph-D « OOSOA » D. Srivastava (2014-2017) INERIS / Univ. Bordeaux

Ph-D « MAOCSA » Y. Zhang (2016-2019) INERIS / LSCE / PSI

LCSQA: National Reference Laboratory for air quality monitoring

CARA program

Funded by the Ministry of Environment

Operated in close collaboration with regional air quality monitoring networks and research lab.

Main goals:

- Describe the nature of pollution episodes
- Identify and quantify the main PM sources
- Quality control / quality assurance within regional networks
- Anticipate new standards and regulations
- Optimize forecasting air quality models

National and European research projects

- EU Intecomp. JRC PMF
- EU FP7 and H2020 ACTRIS
- ADEME CORTEA INACS
- Primequal ZAPA Prequalif
- ADEME R&D SOURCES

INERIS maîtriser le risque pour un développement durable

The CARA program

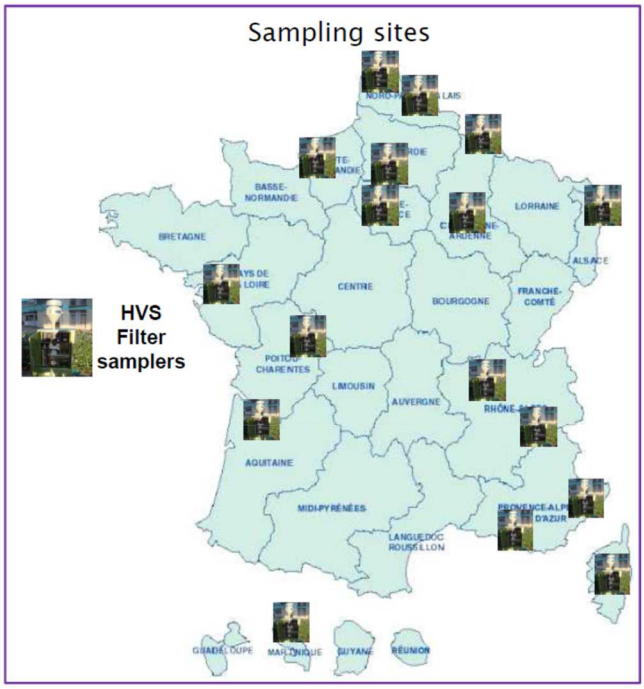

- Settled down by the French reference laboratory for air quality monitoring (LCSQA)
- Since 2008
- To characterize PM chemical composition and sources
- In collaboration with regional networks
- Historically based on filter sampling and off-line analyses (PM_{10} at urban background sites)

INERIS maîtriser le risque pour un développement durable

PM chemical characterization

Filter sampling (usually 24H)

Chemical composition

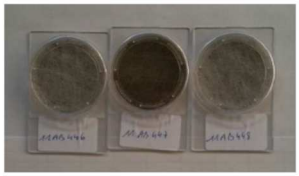

Major chemical species:

- Carbonaceous aerosols : elemental carbon (EC) and organic matter (OM)
- Ions (anions/cations):
  - secondary inorganic aerosols: nitrate, sulfate, ammonium, …
  - Na^+, Cl^-, Mg^{2+} … : sea salts
  - Ca^{2+} : dust
- Some metals:

e.g., Si, Al, Ti, Fe, Ca … → minral dust

Poitiers centre - 2015

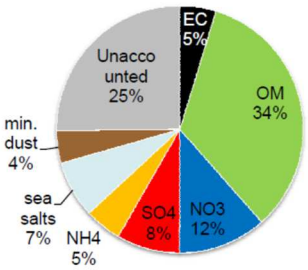

PM chemical characterization

Filter sampling (usually 24H)

Short communication

Assessing in near real time the impact of the April 2010 Eyjafjallajökull ash plume on air quality

Augustin Colette [a,*], Olivier Favez [a], Frédérik Meleux [a], Laura Chiappini [a], Martial Haeffelin [b], Yohann Morille [c], Laure Malherbe [a], Arnaud Papin [a], Bertrand Bessagnet [a],

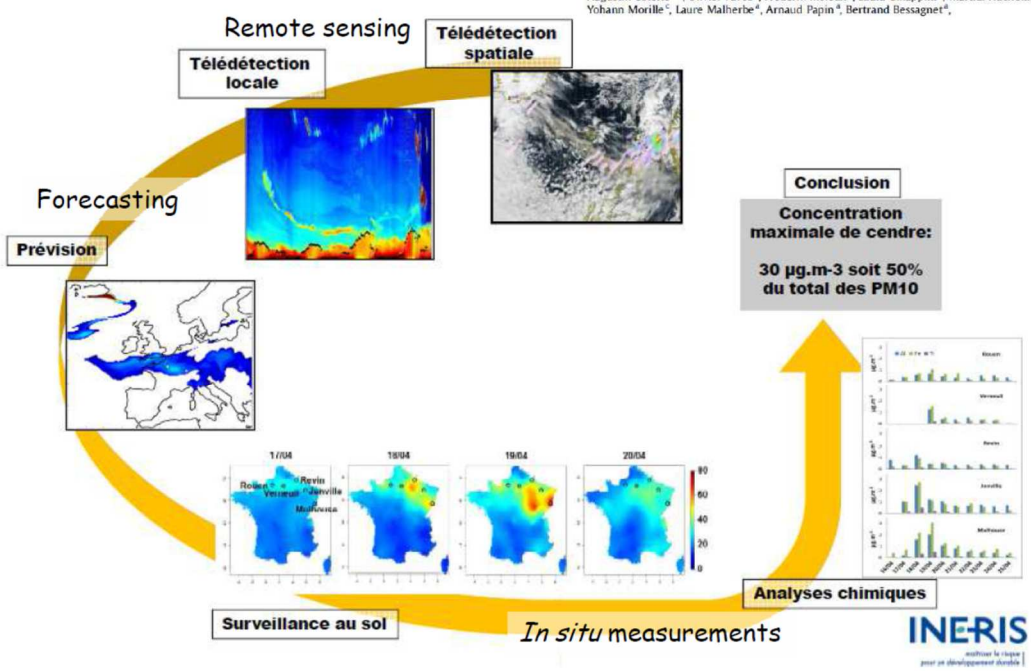

PM source apportionment

Filter sampling (usually 24H)

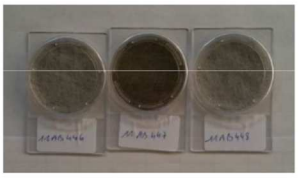

Chemical composition

Source identification and apportionment

Major chemical species

- Espèces carbonées: carbone suie et matière organique
- Ions (anions/cations):
  - espèces inorganiques secondaires: nitrate d'ammonium, sulfate d'ammonium
  - Na^+, Cl^-, Mg^{2+} … : sels de mer
  - Ca^{2+} : dust (poussières terrigènes)
- Métaux majeurs:

Par exemple: Si, Al, Ti, Fe, Ca … → dust

Sources :

- organic markers:
  - sugars: Levoglucosan, mannosan, galactosan → Biomass burning; Arabitol, sorbitol, mannitol → bioaerosols
  - MSA → biogenic marine SOA
  - PAHs (primary & secondary)
  - …
- Trace metals:

E.g., : Ni & V → Heavy oil combustion

PM source apportionment

Filter sampling (usually 24H)

Yearly cycle of organic markers (measured on daily filters sampled every third day)
Poitiers, urban background, 2015

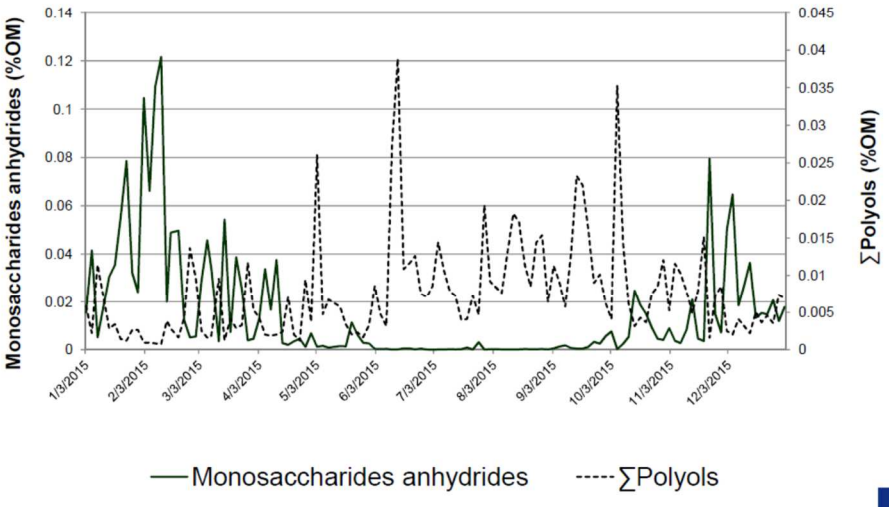

PM source apportionment
Positive Matrix Factorization studies

Receptor modelling approaches:

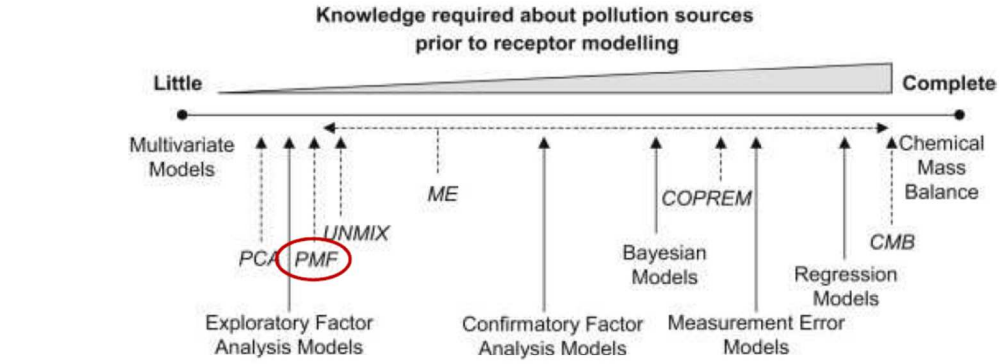

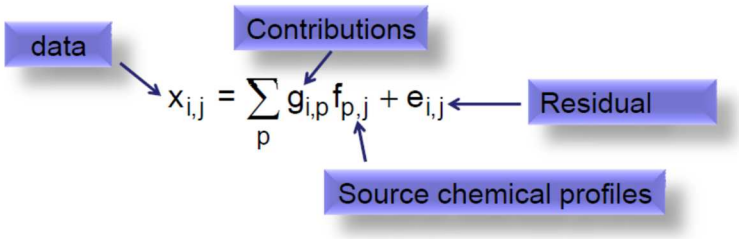

INERIS

PM source apportionment
Positive Matrix Factorization studies

Examples (daily filters sampled every third day):

Rouen (oct. 2010 - oct. 2011)

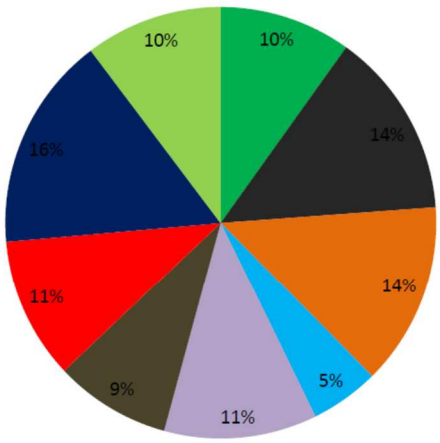

Lens (mars 2011 - mars 2012)

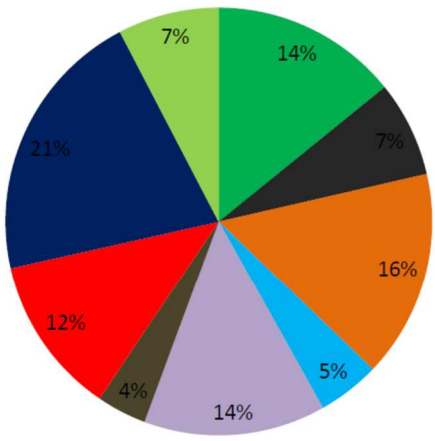

INERIS

PM source apportionment
Positive Matrix Factorization studies

Before 2011 ***2012-2016***

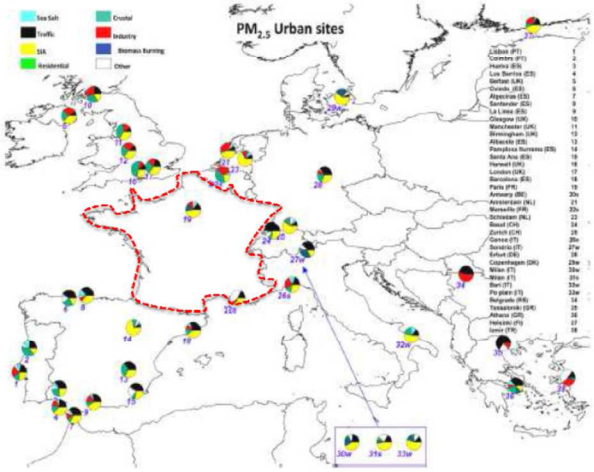

Belis et al., Atmos Env 2013

Current running national research project ('*SOURCES*') to gather, compare and synthetize outputs from these individual studies

Chemical characterization of PM pollution episodes

Filter-based PM chemical speciation

10 largest PM pollution events (2010-2014) at a urban background site (Rouen)

Répartition des espèces chimiques majeures lors des 10 plus importants précédents épisodes de pollution particulaire (au moins 5 jours consécutifs présentant une moyenne globale en PM_{10}>50µg/m³) à Petit-Quevilly (fond urbain, Air Normand):

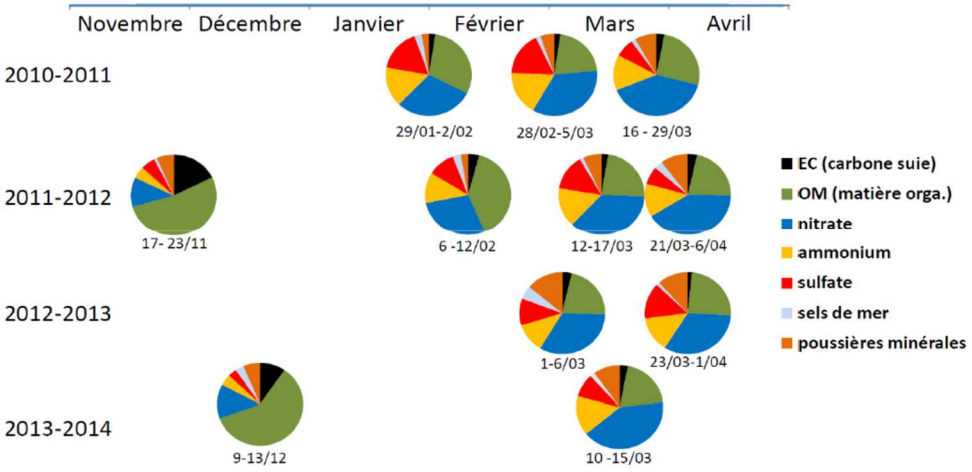

Typical PM pollution episodes

Typical winter PM pollution event

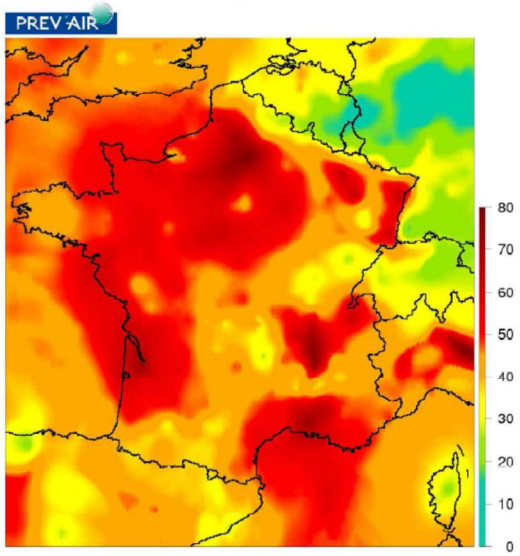

10/12/2013

Typical spring PM pollution event

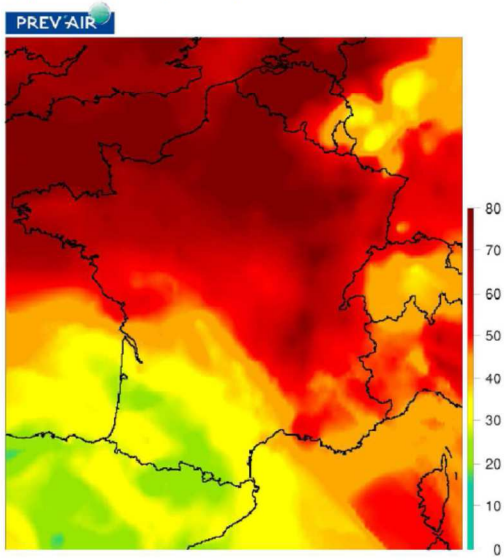

13/03/2014

INERIS
maîtriser le risque pour un développement durable

Early winter pollution episodes

Example: end of December 2014 – early January 2015

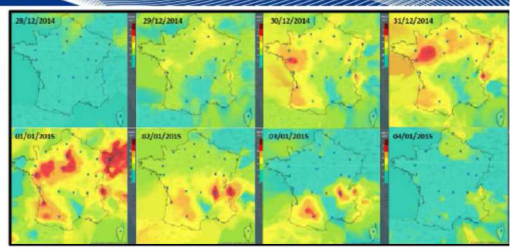

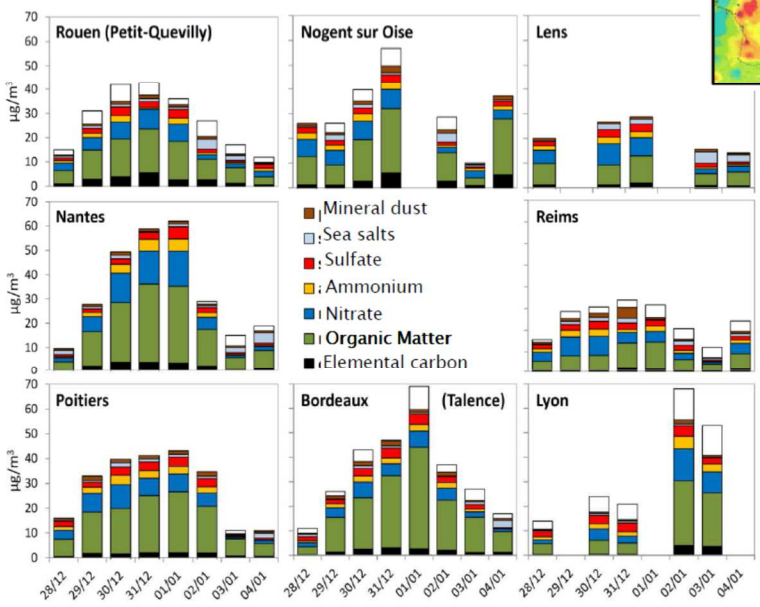

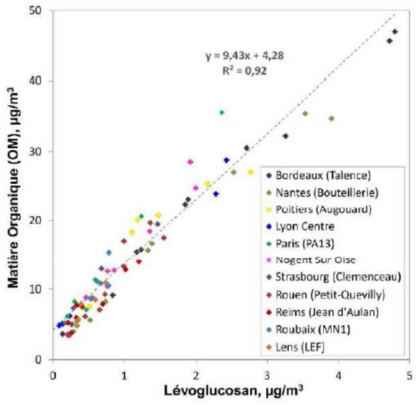

INERIS
maîtriser le risque pour un développement durable

Mono-tracer approaches

E.g. for biomass burning influences

$PM_{biomasse} \approx f \times Levoglucosan$

www.lcsqa.org

Sites	f LCSQA 2014-2015	f Previous study
Rouen	10,9	10,4*
Reims	13,5	
Strasbourg	7,9	
Nantes	10,3	
Poitiers	10,1	
Lyon	12,1	11,4*
Grenoble	11,7	11,9**
Bordeaux	9,1	8,9*
Marseille	*10,7*	
Nice	10,5	

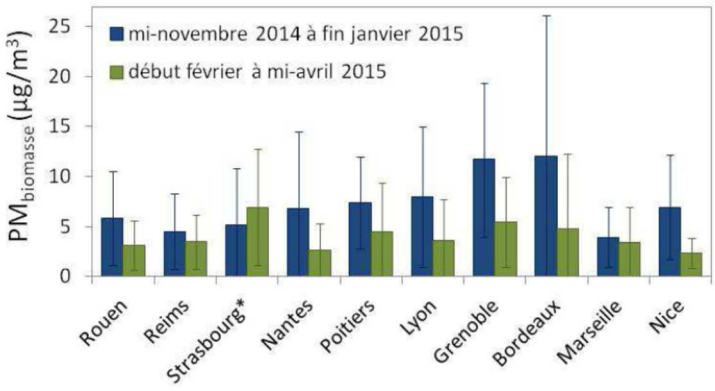

Late winter - early spring pollution episodes

Example of March 2014 episode

Evolution des espèces chimiques majeures au sein des PM_{10} entre le 5 et 16 mars 2014

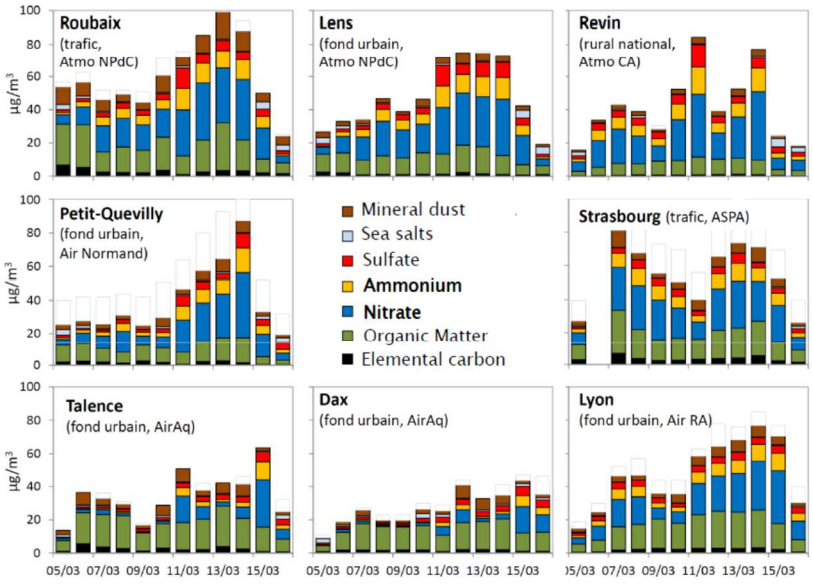

Late winter - early spring pollution episodes

Ammonium nitrate formation mechanisms

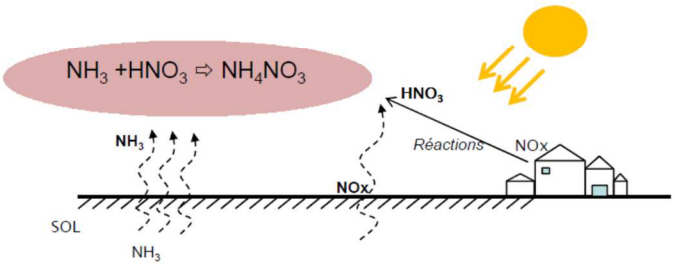

- NH_3 quasi-exclusively coming from agricultural activities
- HNO_3 coming from NOx oxidation
- NO_x mostly emitted by vehicles
- NH_4NO_3 is semi-volatile

Then, what is the main source ?

INERIS
maîtriser le risque pour un développement durable

Sources of ammonium nitrate gaseous precursors

INACS = nationaly-funded project to investigate the interest of measuring stable N and O isotopes

E.g., measuring δ15N in ammonia/ammonium samples…

… at emissions and …

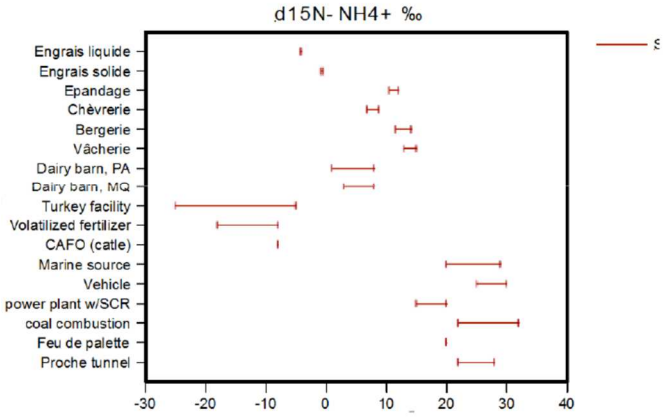

… in ambient air (filters)

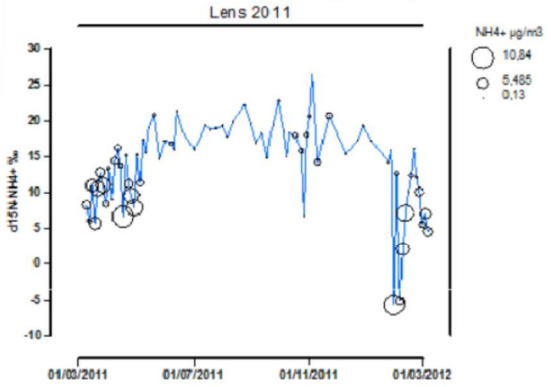

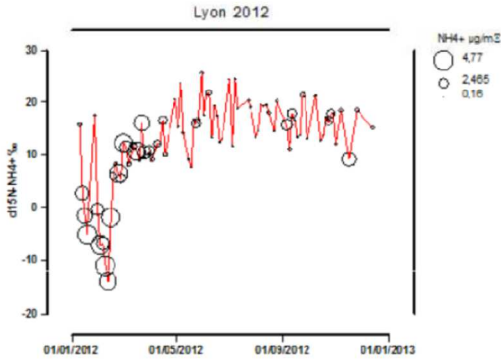

Sources of ammonium nitrate gaseous precursors

INACS = nationaly-funded project to investigate the interest of measuring stable N and O isotopes

E.g., measuring δ15N in ammonia/ammonium samples…

… at emissions and …

d15N- NH4+ ‰

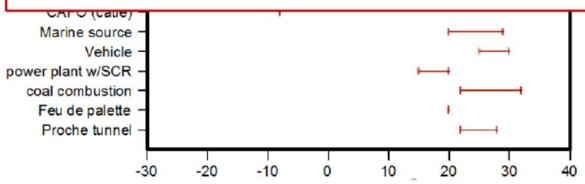

… in ambient air (filters)

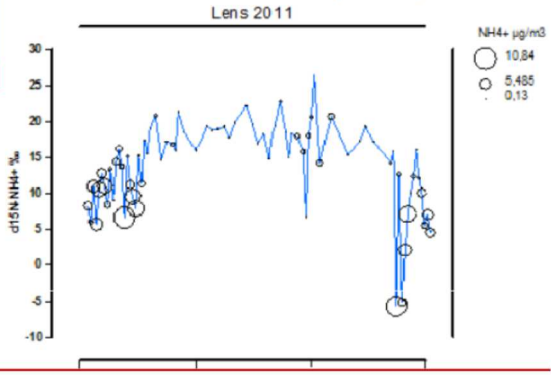

- During early spring pollution episodes, ammonium isotopic signature is quite close to agricultural ammonia emission signatures

- During the rest of the year, ammonia combustion sources could play a more important role than expected

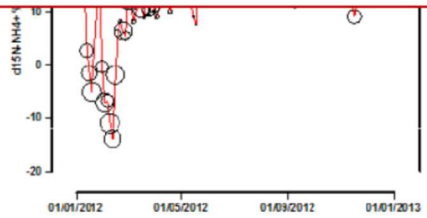

The CARA program

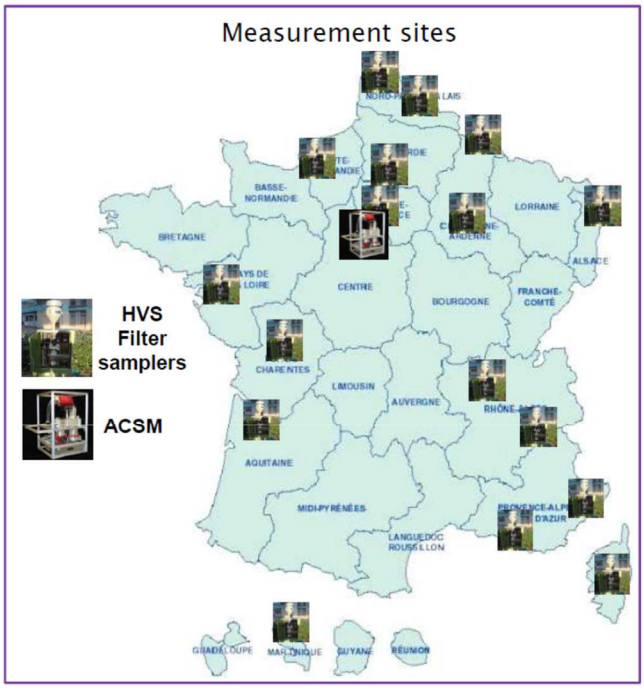

- Public powers asking for data and information in real-time
- Make use of ACSM installed at the SIRTA station since end of 2011

Continuous monitoring of non-refractory submicron aerosol composition by thermal particle vaporization aerosol mass spectrometry (0-200 amu).

Sulfate*, *Nitrate*, *Chloride*, *Ammonium*, *Organics

Example of real-time ACSM measurements

September 2014

Ammonium sulfate aerosols due to volcanic emissions (Iceland) observed at SIRTA using the Aerosol Chemical Speciation Monitor (ACSM, *Aerodyne Res. Inc.*)

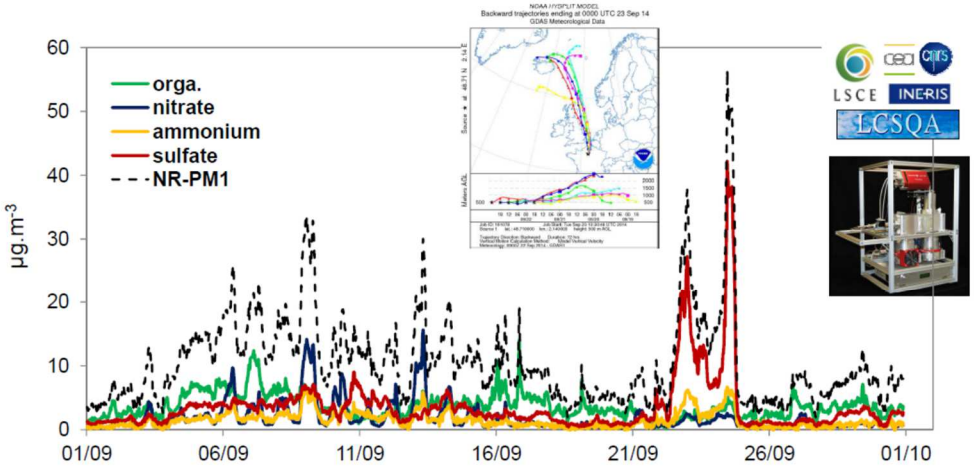

SIRTA regional background site (Paris region)

INERIS maîtriser le risque pour un développement durable

The CARA program

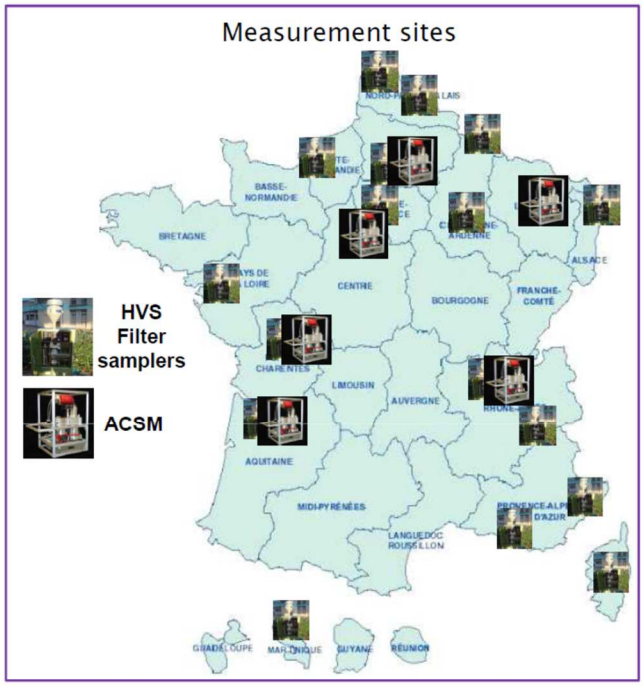

- Public powers asking for data and information in real-time
- Make use of ACSM measurements at the SIRTA station since end of 2011
- 6 ACSM's installed in the last two years by regional air quality monitoring networks

INERIS maîtriser le risque pour un développement durable

The CARA program

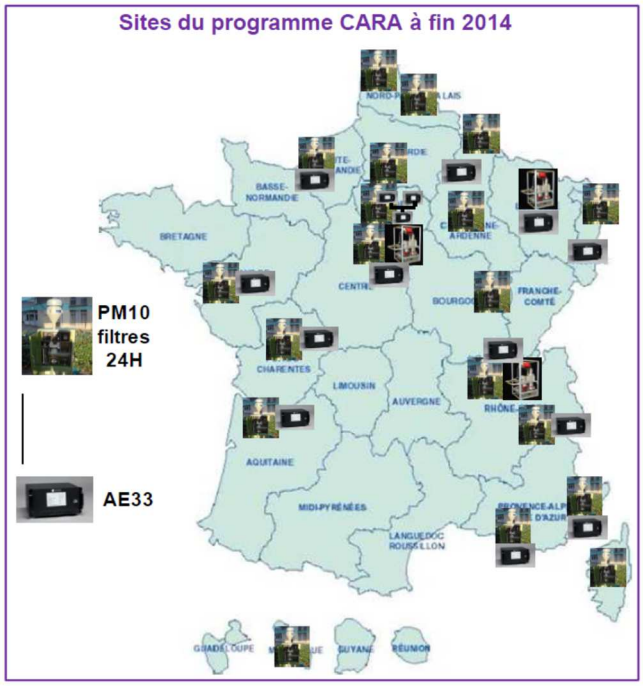

- Public powers asking for data and information in real-time
- Starting implementing multi-wavelength AE33 Aethalometers in 2012

- Monitoring Black Carbon (BC) as an indicator for combustion emissions
- Robust and rather low maintenance costs
- Automatic correction for sampling artefacts
- Allowing to deconvolute:

$$BC = BC_{ff} + BC_{wb}$$

INERIS
maîtriser le risque pour un développement durable

March 2015: PM_1 chemical composition

ACSM + AE33

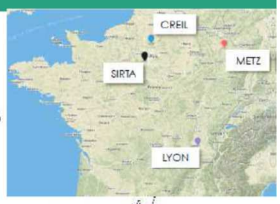

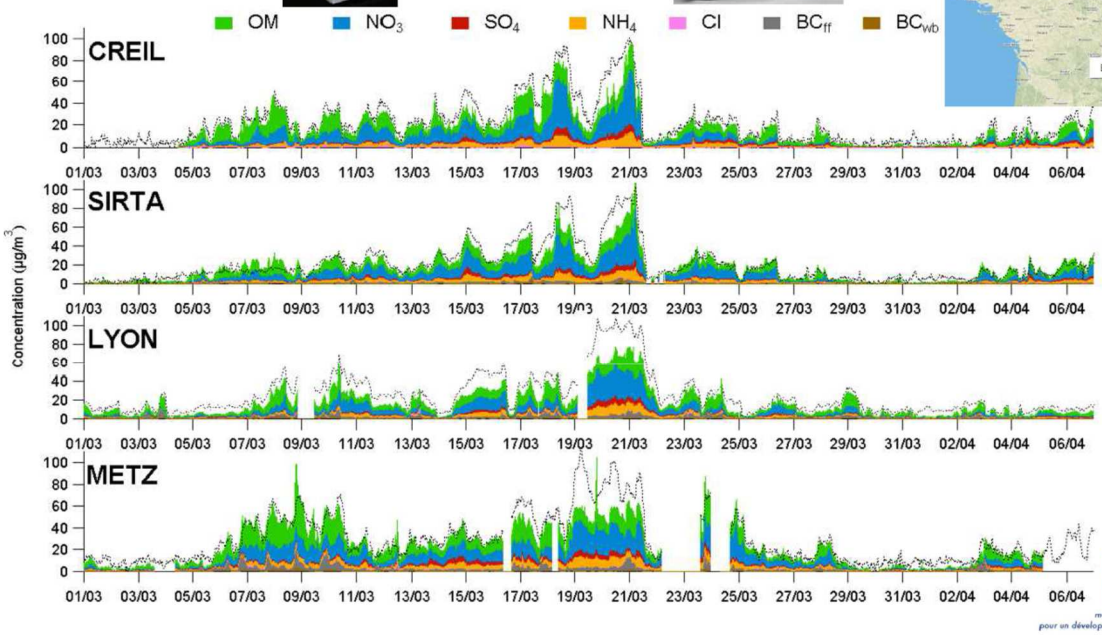

INERIS
maîtriser le risque pour un développement durable

Geographical origins

Percentage of external contributions to total PM_{10}
(Computational simulations using *Chimere*)

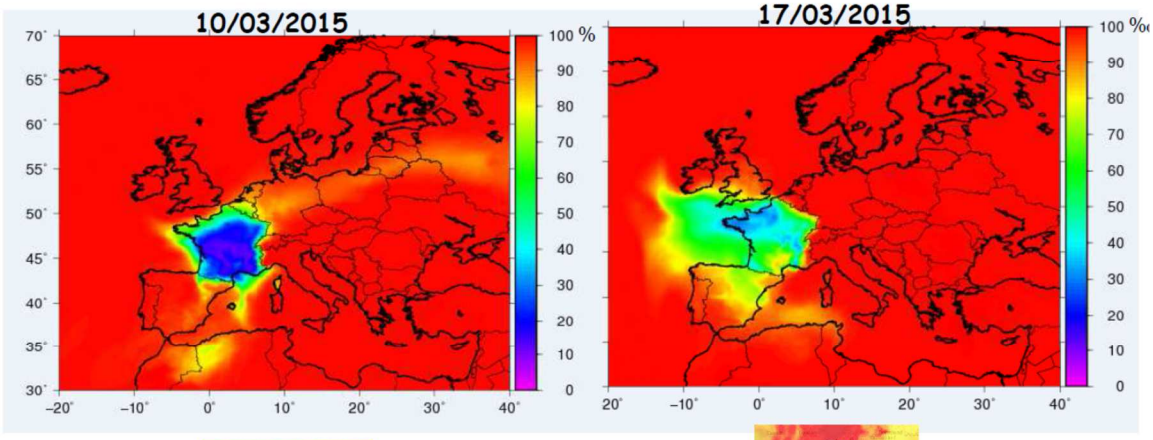

PM10 levels:

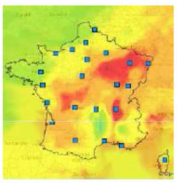

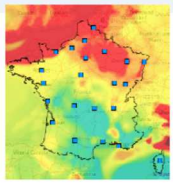

INERIS
maîtriser le risque pour un développement durable

December 2016: PM_1 chemical composition

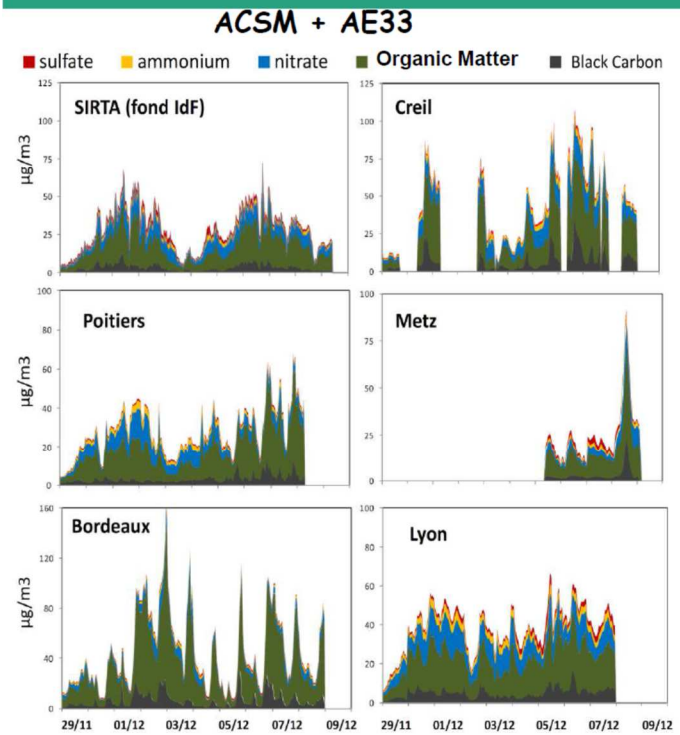

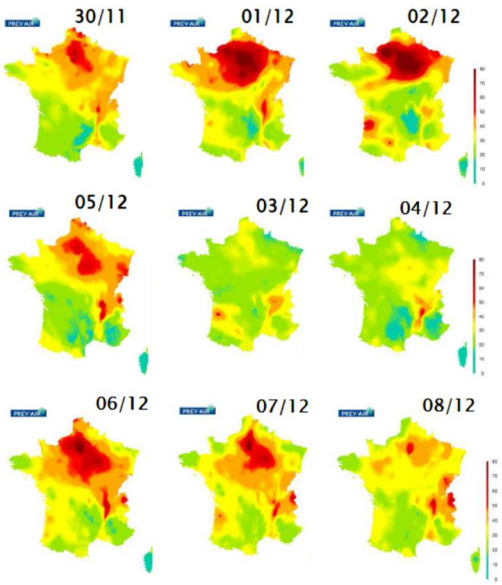

December 2016: Combustion PM

AE33:

$BC = BC_{ff} + BC_{wb}$

And then:

$PM_{wb} = a \times BC_{wb}$

$PM_{ff} = b \times BC_{ff}$

a: from previous campaign(s) at the same sites

b: from literature

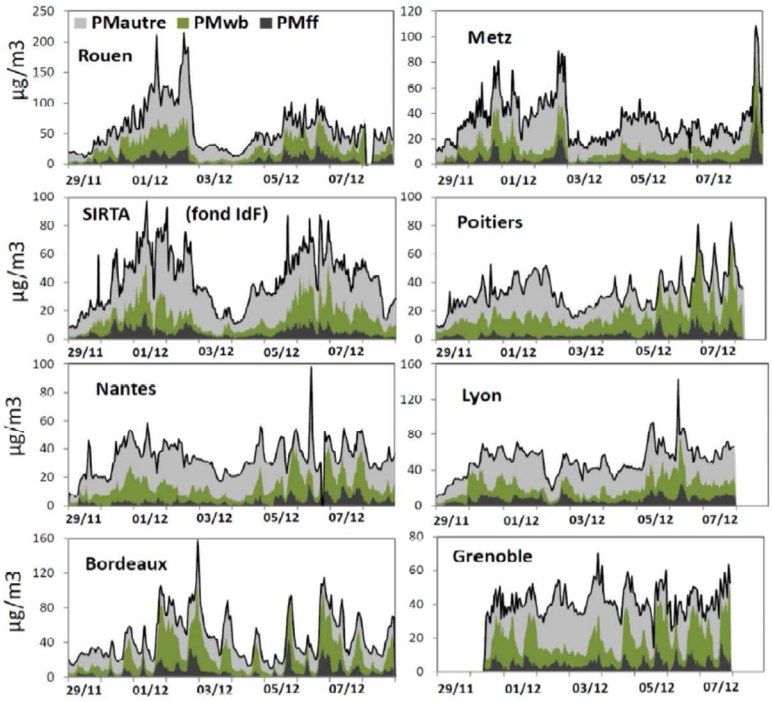

December 2016: PM_{10} composition

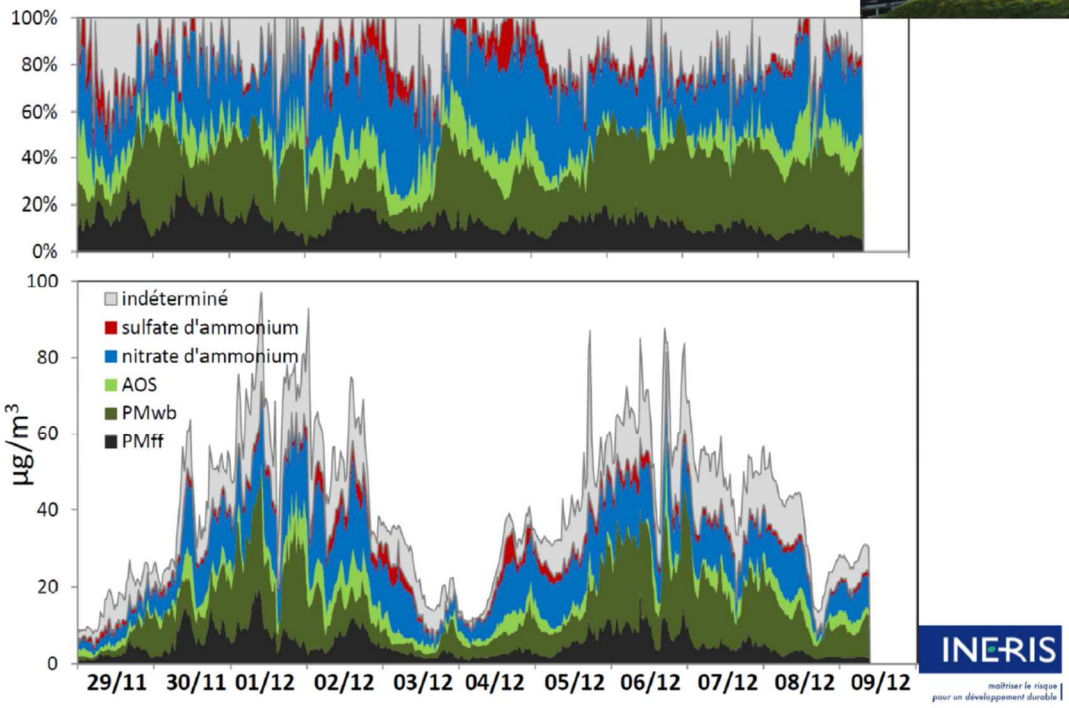

The Aerosol Chemical Monitor Calibration Centre (ACMCC)

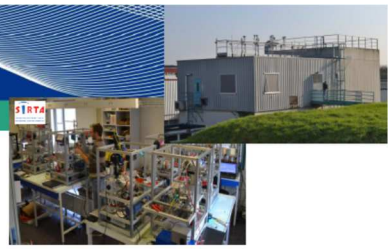

Role:

- Calibration facility for on-line *in-situ* chemical analyzers (ACSM, MARGA, Sunset Field Inst., …)
- Intercomparison studies, audit, training, exchange of knowledge, best-practice

the ACTRIS ACSM network

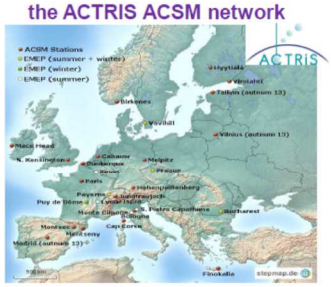

Node: France (CNRS /CEA / INERIS)

Users: Research institutions, (French) national reference laboratory, manufacturers

Added values:

- Support to operational (air quality) agencies
- Towards WMO-GAW World Calibration Center for on-line aerosol chemistry ?

Second ACSM intercomparison exercice (March-April 2016)

2016 ACTRIS-2 ACSM intercomparison exercice at the ACMCC

Goal: Homogenous quality-controlled ACSM datasets at a European scale

- ✓ Intercomparison campaign took place March/April 2016. A total of 21 instruments.
- ✓ In order to accommodate all applications to the intercomparison exercise, two separate calibration exercises were organized.

Participating stations:
Intercomparison Spring 2016

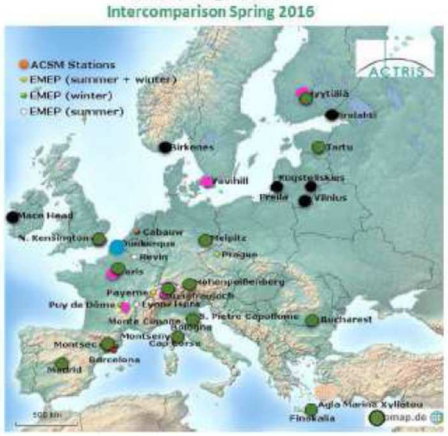

Q-ACSM
ToF-ACSM
HR-AMS
Did Not Attend

Site	Intercomparison	
	Q-ACSM	ToF-ACSM
Hohenpeissenberg		
FMI –Hyytiala		
Cyprus		
Melpitz		
Finokalia		
London		
Bologna		
Madrid		
Vavihill		
SMEAR		
Zurich		
JFJ		
Bucharest		
Barcelona		
PUY		
SIRTA		
CapCorse		
Tartu		
ToFwerk		

Conclusion and perspectives

- ACSM and AE33 are robust instruments for on-line and long-term fine aerosols chemical characterization
- ACMCC should help better operate them on the long-term basis
- Other instruments may be quite approriate to complement the two latter ones
- Filter sample analyses (e.g., stable isotopes) might still be needed for better understanding sources
- To be extented:
  - source apportionment on (long-term) real-time datasets
  - epidemiological studies in combination with these long-term datasets
  - (comprehensive) real-time source apportionment using on-line measurements

INERIS
maîtriser le risque pour un développement durable

Thank you for your attention

And also special thanks to regional air quality monitoring networks in particular for this talk :
- Air Normand,
- Atmo Hauts de France,
- Atmo Grand Est,
- Atmo Auvergne-Rhône-Alpes,
- Air Pays de la Loire,
- Atmo Nouvelle Aquitaine.

INERIS
maîtriser le risque pour un développement durable